BIOLOGICAL SULFUR REACTIONS AND THE INFLUENCE ON FLUID FLOW AT MID-OCEAN RIDGE HYDROTHERMAL SYSTEMS

A Thesis
Presented To
The Academic Faculty

By

Brendan William Crowell

In Partial Fulfillment
Of the Requirements for the Degree
Master of Science in Earth and Atmospheric Sciences

Georgia Institute of Technology

August, 2007

BIOLOGICAL SULFUR REACTIONS AND THE INFLUENCE ON FLUID FLOW AT MID-OCEAN RIDGE HYDROTHERMAL SYSTEMS

Approved by:

Dr. Robert P. Lowell, Advisor
School of Earth and Atmospheric Sciences
Georgia Institute of Technology

Dr. Zhigang Peng
School of Earth and Atmospheric Sciences
Georgia Institute of Technology

Dr. Andrew V. Newman
School of Earth and Atmospheric Sciences
Georgia Institute of Technology

Date Approved: July 7, 2007

ACKNOWLEDGEMENTS

I would like to thank Dr. Robert Lowell for all his guidance and advice over the past two years. If it were not for him taking a chance on me, my direction in life would be completely different. I would also like to thank my other reviewers, Dr. Peng and Dr. Newman. Their comments and help have been invaluable. Also, I would like to thank my fellow geophysics graduate students who have been incredibly friendly and welcoming in my time at Georgia Tech, and they have provided me with many amazing intellectual conversations. I want to thank my family for all of the support they have given me during my life and for pushing me to achieve more than I ever thought. I need to also thank all my friends I have met in my many years at Tech, without whom I would have gone crazy and not had any fun. This work has been supported by the National Science Foundation under grant # OCE-0527208 to Robert P. Lowell and Leonid Germanovich.

TABLE OF CONTENTS

LIST OF TABLES

LIST OF FIGURES

LIST OF SYMBOLS

Symbol	Definition	Value
a	Thermal diffusivity	10^{-6} m^2/s
A	Area	
B	Bacterial count per unit volume of water	
C	Concentration	
c_f	Specific heat of fluid	4000 J/kg^{o}C
d	Depth of subsurface biosphere	
D_{SO_4}	Diffusivity of sulfate	10^{-10} m^2/s
H	Vertical scale of hydrothermal system	1000 m
G	Gibbs free energy	
g	Acceleration due to gravity	9.8 m/s^2
k	Permeability	
K_G	Gibbs energy dissipation coefficient	83 kJ/g C
l	Length scale	
m_{H_2S}	Molar mass of hydrogen sulfide	34 g/mol
Q	Mass flow rate	
Ra	Rayleigh number	
r_{floc}	Radius of floc cylinders	1.0 μm
t	Time	
T	Temperature	
T_o	Temperature of bottom of hydrothermal system	400 ^{o}C
U	Specific discharge (Darcian velocity)	
V	Volume	
v_z	Velocity in the vertical direction	
x	Mixing ratio of high temperature fluid and seawater	
X_{floc}	Maximum growth rate of floc	3 μm/min
y	Height of vertical boundary	
z	Vertical Cartesian coordinate	
β	Coefficient of thermal expansion	10^{-3} ^{o}C^{-1}
δ	Boundary layer thickness	
λ_m	Thermal conductivity	2.5 W/m^{o}C
ν	Kinematic viscosity	10^{-7} m^2/s
ρ_f	Density of fluid	1000 kg/m^3
ρ_{floc}	Density of floc	2000 kg/m^3
Φ	Porosity	0.1

SUMMARY

This thesis is an investigation into biogenic sulfide oxidation and sulfate reduction associated with hydrothermal systems at oceanic spreading centers. Hydrogen sulfide oxidizing bacteria have been shown to produce filamentous sulfur in the laboratory. At mid-ocean ridges following magmatic eruptions the filamentous sulfur appears in the form of floc that emerges during 'snowblower' events. Sulfur floc production is estimated in two ways. First, the hydrogen sulfide flux from high temperature vents is compared to the adjacent diffuse flow to estimate the rate of sulfur production in the shallow crust since the 1991 eruption between 9 and 10 °N on the East Pacific Rise (EPR). Secondly, data from laboratory experiments is used to provide an upper estimate of sulfur floc production during a volcanic eruption. The calculations suggest that the porosity change due to sulfur floc production is relatively small over the period between the 1991 eruption and the recent eruption in late 2005, even though floc is being stored in the pore space. Based on calculations for the EPR, the floc observed during 'snowblower' events is most likely a combination of a bloom event and floc that has been stored in the crust in the years between eruption cycles. Sulfate reducing bacteria follow an extremely important metabolic pathway and are found in all oceans and lakes, and in particular at deep-sea hydrothermal systems. Seawater sulfate plays a vital role at hydrothermal vents because much of the sulfide at vents comes from the reduction of seawater sulfate, primarily as a result of basalt-seawater reactions. Also of importance is the precipitation of anhydrite ($CaSO_4$) at hydrothermal vent recharge zones, which could potentially clog pore-space, thus reducing the porosity and changing the overall dynamic structure of the hydrothermal system. Likewise biogenic sulfate reduction during hydrothermal recharge may limit the amount of anhydrite precipitation.

Biogenic sulfate reduction is investigated by deriving a theoretical sulfate reduction rate curve with respect to temperature, based on laboratory experiments on sediment cores from the Guaymas Basin in the Gulf of California, and then applying the results to the temperature profile of the system. Although biogenic sulfate reduction calculated in this manner may be applicable to regions of upflow within the Guaymas Basin, the rate appears to be orders of magnitude too high when it is applied to Guaymas Basin cores characterized by recharge and to hydrothermal recharge zones at mid-ocean ridge axes. In part, this is because the sediment cores were taken from a zone of pore water upflow in which very large thermal gradients are present so sulfate reduction occurs on a very small spatial scale. Another factor stems from the fact that Guaymas basin sediments are greatly enriched in organic matter and nutrients that may promote sulfate reduction. These factors are absent at sediment bare mid-ocean ridges. Estimates of biogenic sulfate reduction from a Gibbs free-energy calculation suggests that the sulfate reduction rate calculated from the upflow cores from Guaymas Basin is about 9 orders of magnitude greater than the estimated worldwide average on mid-ocean ridge flanks. The rate from the upflow cores appears to be at least two orders of magnitude greater than in the recharge cores from the Guaymas Basin. The role of diffusion is shown to have almost no effect on biogenic sulfate reduction. Slower flow speeds allow for more biogenic sulfate reduction due to the longer residence time of fluids in the system and faster flow speeds have a negligible amount of biogenic sulfate reduction. However, faster flow speeds allow for a greater percentage of pore space to be filled by the precipitation of anhydrite and the precipitation of anhydrite at very low speeds provides almost no clogging of porosity. This is important because biogenic sulfate reduction removes sulfate that would otherwise be utilized for anhydrite precipitation, reducing the amount of anhydrite precipitated.

CHAPTER 1

INTRODUCTION

The discovery of seafloor hydrothermal vents at the Galapagos Rift in 1977 [*Corliss et al*., 1979] changed the overall understanding of life on Earth and the extremes at which organisms can thrive. The overall biomass and diversity of life found at deep-sea hydrothermal vents is estimated to be many orders of magnitude greater than the biomass found at other sites at similar depths and they represent ecosystems that are completely independent of solar energy [*Jannasch*, 1985]. Microorganisms at hydrothermal vent sites exist in tremendous thermal and chemical gradients between the ~400 ^{o}C black smoker fluids and the 2 ^{o}C seawater [*Chevaldonne and Godfroy*, 1997]. Biological, chemical and physical processes alter the composition of both the circulating seawater and the oceanic crust in a dynamical two-way exchange of chemical species [*Lowell et al.*, 1995]. Of particular interest is the symbiotic relationship between the microorganisms, which thrive by chemosynthesis of CO_2 into organic carbon compounds, and the higher life forms at hydrothermal vents [*Jannasch and Mottl*, 1985]. Seafloor hydrothermal systems follow many of the same trends in invertebrate-symbiont relationships such as sulfide and carbon dioxide uptake, transport, toxicity, pH regulation, carbon-fixation and nitrogen metabolism [*Van Dover and Lutz*, 2004]. This complex balance of energy in an extreme environment has led many to speculate that seafloor hydrothermal systems could have been the location for the origin of life on Earth [*Corliss et al*., 1981; *Baross and Hoffman*, 1985]. The possibility of hydrothermal systems existing on other planetary bodies such as Europa and Titan has given rise to much conjecture into the existence of life elsewhere in the solar system [*Chyba*, 2000; *Chyba and Phillips*, 2001; *McKay and Smith*, 2005].

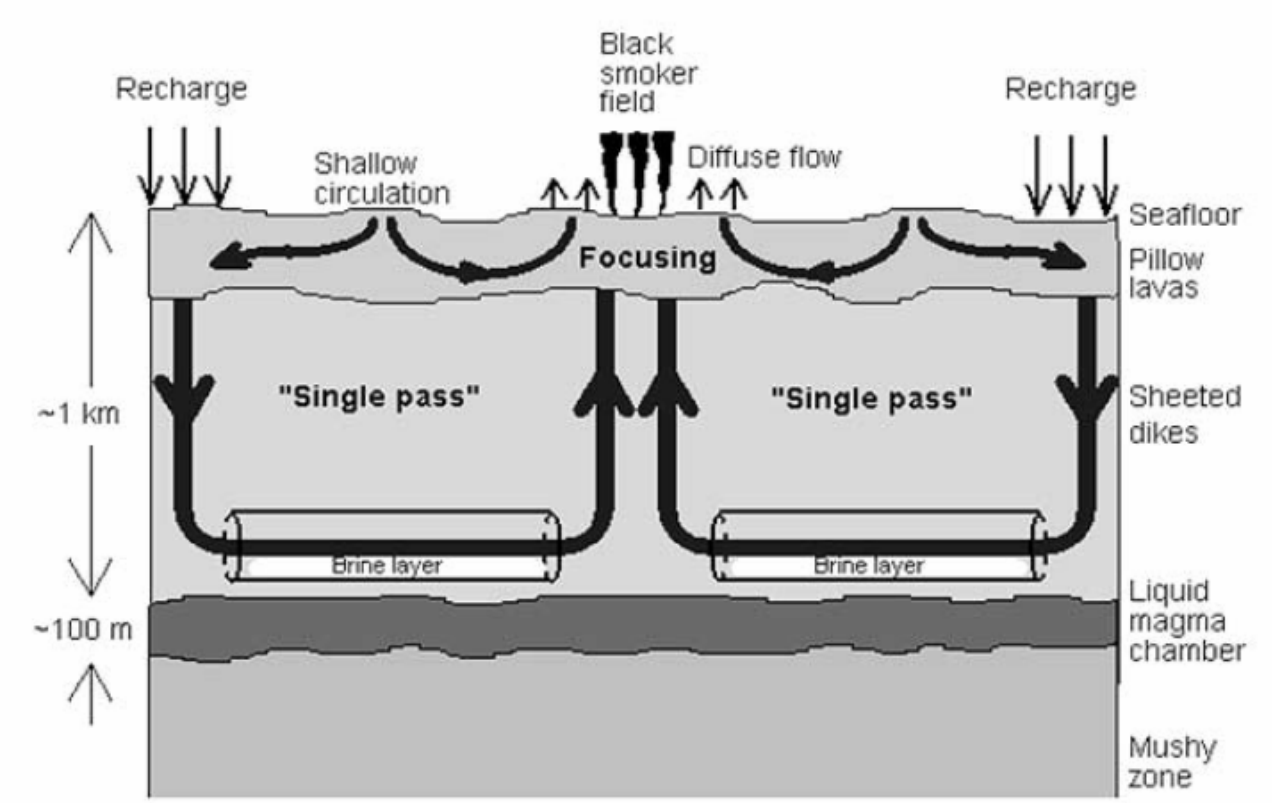

Figure 1.1: Schematic of a single-pass model for hydrothermal circulation [from *Lowell and Germanovich*, 1997]

Seafloor hydrothermal vents can be categorized into low temperature (10-30 ^{o}C), low flow rate diffuse vents, or high temperature (300-400 ^{o}C), highly focused flow vents [*Jannasch and Mottl*, 1985]. The interplay between the diffuse flow, focused flow and seawater is very complex and poorly understood due to the challenges of modeling heat flow, chemical transport and the evolution of crustal permeability for the complete hydrothermal system [*Lowell and Germanovich*, 2004]. Both single-pass and cellular convection models have been used to investigate hydrothermal circulation [see reviews by *Lowell*, 1991; *Lowell et al.*, 1995; *Fisher et al.*, 2003; *Lowell and Germanovich*, 2004; *Lowell et al.*, 2007*a*]. An example of a single-pass model is presented in Figure 1.1. The processes by which ascending high temperature fluids become focused are poorly understood, and in some instances the flow does not focus at all [e.g.,

Lowell et al., 2003; Lowell et al., 2007b]. At 9°47'N on the East Pacific Rise (EPR), the flow started at 78 °C following the 1991 eruption and over the course of 10 years, the flow became focused into a high temperature black smoker vent [*Von Damm*, 2000]. *Lowell et al.* [2003] proposes that the precipitation of anhydrite ($CaSO_4$) may be a potential focusing mechanism in the evolution of high temperature vents.

Although there has been considerable effort devoted to modeling physical and chemical processes in seafloor hydrothermal systems, much less attention has been directed towards modeling biological process or linking biological processes to physical processes. This thesis addresses two important problems linking biological and physical processes in seafloor hydrothermal systems. The two problems are encountered in two separate parts of the hydrothermal system. One problem concerns the oxidation of hydrogen sulfide from vent fluids ascending through the shallow crust, the formation of 'snowblower' vents, and the evolution of permeability in the shallow crust. The second problem concerns the possible importance of biogenic reduction of seawater sulfate during hydrothermal recharge and its possible role in affecting the porosity and permeability of recharge.

1.1: 'Snowblowers' and Sulfide Oxidation

The presence of hydrogen sulfide (H_2S) at seafloor hydrothermal systems is crucial to the existence of large biological communities. Sulfide dominates the speciation of sulfur in mid-ocean ridge basalt magmas and there is insignificant sulfur loss during the cooling of magma due to a lack of SO_2 degassing [*Bach and Edwards*, 2003]. There are two potential sources of H_2S at hydrothermal vents. The first is from the leaching of sulfide from crustal basalt and the second is

from the reduction of seawater sulfate along with the oxidation of Fe^{2+} into Fe^{3+} from basalt [*Jannasch and Mottl*, 1985].

Table 1.1: An overview of metabolic processes at seafloor hydrothermal vents

Electron Donor	Electron Acceptor	Metabolic Process
S^{2-}, S^{o}, $S_2O_3^{2-}$, $S_4O_6^{2-}$	O_2, NO_3^-	Sulfur Oxidation, Denitrification
H_2	O_2, NO_3^-	Hydrogen Oxidation, Denitrification
H_2	S^{o}, SO_4^{2-}, $S_2O_3^{2-}$	Sulfur/Sulfate Reduction
Fe^{2+}, Mn^{2+}	O_2	Iron/Manganese Oxidation
NH_4^+, NO_2^-	O_2	Nitrification
CH_4	O_2	Methanotrophy
H_2	CO_2	Methanogenesis
CH_4	SO_4^{2-}	Methane Oxidation
Organic Compounds	S^{o}, SO_4^{2-}	Sulfur/Sulfate Reduction

Table adapted from *Jannasch and Mottl* [1985] and *Kelley et al.* [2002].

The shallow mixing zones and the diffuse flow areas are some of the most interesting areas biologically due to high concentrations of sulfide. Diffuse flow vents at active hydrothermal vents contain ~10^5 microorganisms per ml which range from sulfur oxidizers, iron oxidizers and methanogens [*Huber et al.*, 2003]. Table 1.1 shows the variety of metabolic activity at seafloor hydrothermal vents. Visual observations of submarine eruptions, such as the 1989 MacDonald seamount and the 1991 9^{o}N EPR events, first revealed evidence of a vast, diverse biosphere of organisms living in fissures, cracks and the subsurface [*Huber et al.*, 1990; *Haymon et al*., 1993; *Embley et al*., 1995; *Holden et al*., 1998]. Following the MacDonald seamount eruption, a number of H_2-oxidizing and sulfur-reducing hyperthermophiles were found in samples taken up to a kilometer away from the seamount [*Huber et al.*, 1990]. The eruption at 9^{o}N EPR involved the expulsion of massive amounts of microbial mats and involved one of the first observations of a 'snowblower' vent, which is a snowstorm of white filamentous sulfur 'floc' that is composed primarily of elemental sulfur and a small percentage of combustible

organic material [*Haymon et al.*, 1993; *Taylor and Wirsen*, 1997]. 'Snowblower' events, the production of sulfur floc and its effects on the porosity structure of the hydrothermal system are further discussed in Chapter 2. The material in this Chapter has been submitted for publication [*Crowell et al.*, 2007]

1.2: Biogenic Sulfate Reduction

Chapter 3 is an investigation into the role of biological sulfate reduction at deep-sea hydrothermal systems. In particular, it looks at the role of biogenic sulfate reduction in recharge zones and how it is related to the mass flow rate. Also interrelated with this is the role of anhydrite precipitation and how biological sulfate reduction affects the available amount of sulfate to be precipitated.

Sulfate reduction rates from ODP sediment cores at Guaymas Basin, Gulf of California [*Jorgensen et al.*, 1992] provide a starting point for the modeling of biogenic sulfate reduction in recharge zones. The sulfate reduction rates as a function of temperature in sediment cores from Guaymas Basin are obtained for a temperature profile that represents hydrothermal discharge, and the majority of sulfate reduction takes place within a thin boundary layer. Moreover, Guaymas basin sediments are rich in organic matter and nutrients, which tend to promote sulfate reduction. These factors lead to reduction rates that are many orders of magnitude larger than what would be expected from hydrothermal recharge zones. A Gibbs free energy approach by *Bach and Edwards* [2003] gives an average sulfate reduction rate of 1.3×10^{-12} mol SO_4/m^3s for the flanks of mid-ocean ridges. This provides the constraint necessary to use the Guaymas Basin data effectively for a recharge zone.

Lowell and Yao [2002] provide an analysis on the pore sealing times due to anhydrite precipitation for hydrothermal recharge zones given a range of flow speeds. This creates a unique coupling between flow speed and the relative importance of biogenic sulfate reduction because when flow speeds are high, there would be appreciable precipitation of anhydrite and minimal biogenic sulfate reduction. However, when the flow speeds are low, anhydrite precipitation may be negligible, but biogenic sulfate reduction may be important. Therefore, biogenic sulfate reduction is not likely to inhibit anhydrite precipitation because the two processes are not important under similar fluid flow conditions.

CHAPTER 2

'SNOWBLOWER' VENTS AND SULFIDE OXIDATION

2.1: Introduction

One of the most striking phenomena associated with seafloor volcanic eruptions and hydrothermal processes is the emission of large quantities of biogenic material commonly referred to as 'floc'. White, biogenic deposits on glassy basalts were discovered two years following the 1986 event plume on the Cleft Segment of the Juan de Fuca Ridge (JDF) [*Embley and Chadwick.*, 1994], and thermophiles were found in sea-water samples following the eruption of Macdonald Seamount in 1989 [*Huber et al.*, 1990]. The first 'live' detection of biogenic emissions occurred in 1991 by a team aboard the *Alvin* submersible at the 9^{o}N site on the East Pacific Rise [*Haymon et al*., 1993]. The team was onsite shortly after a volcanic eruption and witnessed widespread outpouring of high-temperature hydrothermal fluids through a network of seafloor cracks and fissures. Hydrogen sulfide and iron concentrations immediately following the eruption were shown to be incredibly high, supplying vent ecosystems with a seemingly endless supply of nutrients [*Shank et al.*, 1998]. Filamentous bacterial mats up to several meters thick covered the fresh basalt flows, and fragments of mat material were carried upward by the hydrothermal flow forming a biogenic 'blizzard' reaching heights of 50 m above the seafloor [*Haymon et al.*, 1993]. They coined the term 'snowblower' vents to describe the hydrothermal flushing of biogenic material from beneath the seafloor. The filamentous biogenic material or 'floc' was later found to be composed primarily of inorganic elemental sulfur [*Nelson et al.*,

1991]; and later laboratory experiments suggested that such sulfur-rich filaments could be excretions produced by H_2S-oxidizing bacteria living near oxic-anoxic interface [*Taylor and Wirsen*, 1997]. *Taylor et al.* [1999] report evidence of rapid *in situ* biogenic production of filamentous sulfur in a warm water hydrothermal vent at the 9°N vent field on the EPR. Early observations of flocculent sulfur discharge following the 1991 eruption place the thickness of sulfur deposited on the seafloor around 5 cm over many areas along the EPR from 9°45' to 9°52'N [*Taylor and Wirsen*, 1997]. Biogenic particles from the 'snowblower' event of 1991 were identified at least 100 m from the west side of the Axial Summit Caldera [*Haymon et al*., 1993]. Floc emission and microbial mats were also observed following the eruption in the same region after the 2005 eruption [*Shank et al.,* 2006].

Observations similar to those on the EPR were made following the diking and eruptive event on the CoAxial Segment of the JDF in 1993 [*Embley et al.*, 1995; *Holden et al.*, 1998]. In a region referred to as Floc, fragments of bacterial mat material rose to heights of 200 m above the seafloor for hundreds of meters across the axial valley [*Embley et al.*, 1995; *Holden et al.*, 1998; *Delaney et al.*, 1998]. Bacterial mats covered the seafloor near the Floc site. The floc from the CoAxial event plume covered between 7 and 14% of the seafloor around the hydrothermally active part of the new lava flow [*Juniper et al.*, 1995]. The floc formed small drifts on the seafloor hundreds of meters west of the central of the axial valley at the Floc site [*Embley et al.,* 1995]. Although the venting temperatures were < 50°C, sulfur-reducing and methanogenic thermophilic and hyperthermophilic organisms were cultured from the fluids [*Holden et al.*, 1998], indicating that these organisms grew in a higher temperature environment beneath the seafloor. Studies of the floc material from the CoAxial segment revealed that they were composed of filamentous, coccoid and rod-shaped forms that were coated with Fe and Si

[*Juniper et al.*, 1995]. Within a year following the CoAxial event, most of the filamentous sulfur material had completely disappeared, most likely due to invertebrate grazing or some unknown mechanism [*Juniper et al.,* 1995]. Filamentous sulfur oxidizing bacteria have also been cultured from microbial mats on sediment layers and in between tube worms at the Guaymas Basin hydrothermal system [*Jannasch et al.*, 1989].

Although there is no doubt that 'floc' emission following these eruptive events is biogenic in origin, the time scale on which it is being created in the sub-seafloor is unclear. Also unclear is the extent to which the floc emitted in 'snowblower' vents represents: (*a*) a microbial 'bloom' following a pulse of nutrients triggered by the magmatic event and enhanced hydrothermal flow or (*b*) a sudden release of floc that has formed and been stored within the shallow crust over a considerable time. In conjunction with (*b*) is the question of whether the production and storage of floc substantively alters the porosity and permeability of the shallow crust and the evolution of the hydrothermal system.

In this chapter, these questions are addressed by two different methods. One method uses the high-temperature and diffuse-flow geochemical data for H_2S, Si, Mg, Cl and Fe that has been obtained over a number of years [*Von Damm and Lilley*, 2004] to estimate flux of H_2S in diffuse flow and the fraction of H_2S used by the biota. This determines the rate of generation of sulfur floc in the shallow oceanic crust, and hence determines whether a 'snowblower' discharge can represent a flushing out of floc that has been stored over a considerable time. By calculating the rate of growth of sulfur floc, its impact on the porosity and permeability of the shallow oceanic crust following the 1991 eruption at 9°N on the EPR can be ascertained. To calculate the rate of sulfur floc production, laboratory measurements on the filamentous sulfur are utilized, showing that the sulfur floc is composed of about 75% elemental sulfur by dry weight and 25%

combustible organic matter [*Taylor et al*., 1999]. In the second method, laboratory data from *Taylor and Wirsen* [1997] and *Taylor et al.* [1999] is used to estimate the composition and growth rate of the sulfur floc to obtain a maximum growth rate of filamentous sulfur. Here the flocculent material is approximated to be cylindrical in shape, with diameters from 0.5 μm to 2.0 μm and a length of 20 μm to 500 μm [*Wirsen et al*., 2002]. Under idealized conditions of hydrogen sulfide, oxygen and carbon dioxide, the filamentous sulfur can be grown at rates > 3 μm/min [*Taylor and Wirsen*, 1997]. This analysis will provide a lower limit on the time scale for the development of a 'snowblower' event as a microbial bloom.

The calculations suggest that the amount of floc observed during the 1991 'snowblower' event may have been created by an incredibly strong bloom event. However, it was most likely a combination of floc being stored in residence and a bloom, or it could have been completely stored in residence and flushed during the magmatic event given enough floc can be created to match the observed 'snowblower' event.

2.2: Methodology and Results

2.2.1: Quasi Steady State Floc Production

In order to estimate the rate of sulfur floc production in the shallow oceanic crust, an array of chemical data from 9^{o} N on the EPR on high-temperature and diffuse-flow fluids obtained between 1991 and 2000 is used [*Von Damm and Lilley*, 2004]. The data came from the Northern and the Southern Transects (Figure 2.1). There are diffuse and high temperature flow data for seven days between April 1991 and April 2000 on the Northern Transect, and there are

data for five days between February 1992 and April 2000 on the Southern Transect. Data from the Middle Transect are not used since diffuse and high temperature data exists for only two days during the time range. The Northern Transect includes the BIO9, BIO9Riftia and the Hole-to-Hell sites. The Southern Transect includes only Tube Worm Pillar (TWP), and therefore data from the Southern Transect will be more consistent over the ten year period because the data comes from a single site rather than being averaged over several vents. The chemical data for the Northern and Southern Transects are listed in Table 2.1.

Table 2.1: Summary of Fluid Data used for creation of floc model

Date	Location	Type of Flow	Max H_2S (mmol)	Max Si (mmol)	Max Fe (µmol)
Apr-91	NT	High Temp	23.2	9.9	2190
		Diffuse	0.901	0.879	151
Dec-93	NT	High Temp	7.3	11.3	1060
		Diffuse	0.276	0.568	24.2
Mar-94	NT	High Temp	8.5	12.6	1430
		Diffuse	0.271	0.786	25
Oct-94	NT	High Temp	6.2	14.1	2730
		Diffuse	0.106	0.923	69.9
Nov-95	NT	High Temp	6.7	14.8	6030
		Diffuse	0.188	1.140	277
Nov-97	NT	High Temp	8.6	13.4	6640
		Diffuse	0.003	0.722	170
Apr-00	NT	High Temp	8.3	11.8	3820
		Diffuse	0.044	0.765	77.2
Feb-92	ST	High Temp	20.7	12.7	4080
		Diffuse	0.660	0.692	2
Oct-94	ST	High Temp	14.3	12.5	1590
		Diffuse	0.206	0.660	11.5
Nov-95	ST	High Temp	14	13.8	1550
		Diffuse	0.531	0.848	9.9
Nov-97	ST	High Temp	11.3	16.1	742
		Diffuse	0.239	0.565	27
Apr-00	ST	High Temp	11.2	16.8	517
		Diffuse	0.055	0.232	23
Seawater	NA	NA	0.000	0.155	0.0005

Table adapted from *Von Damm and Lilley*, 2004.

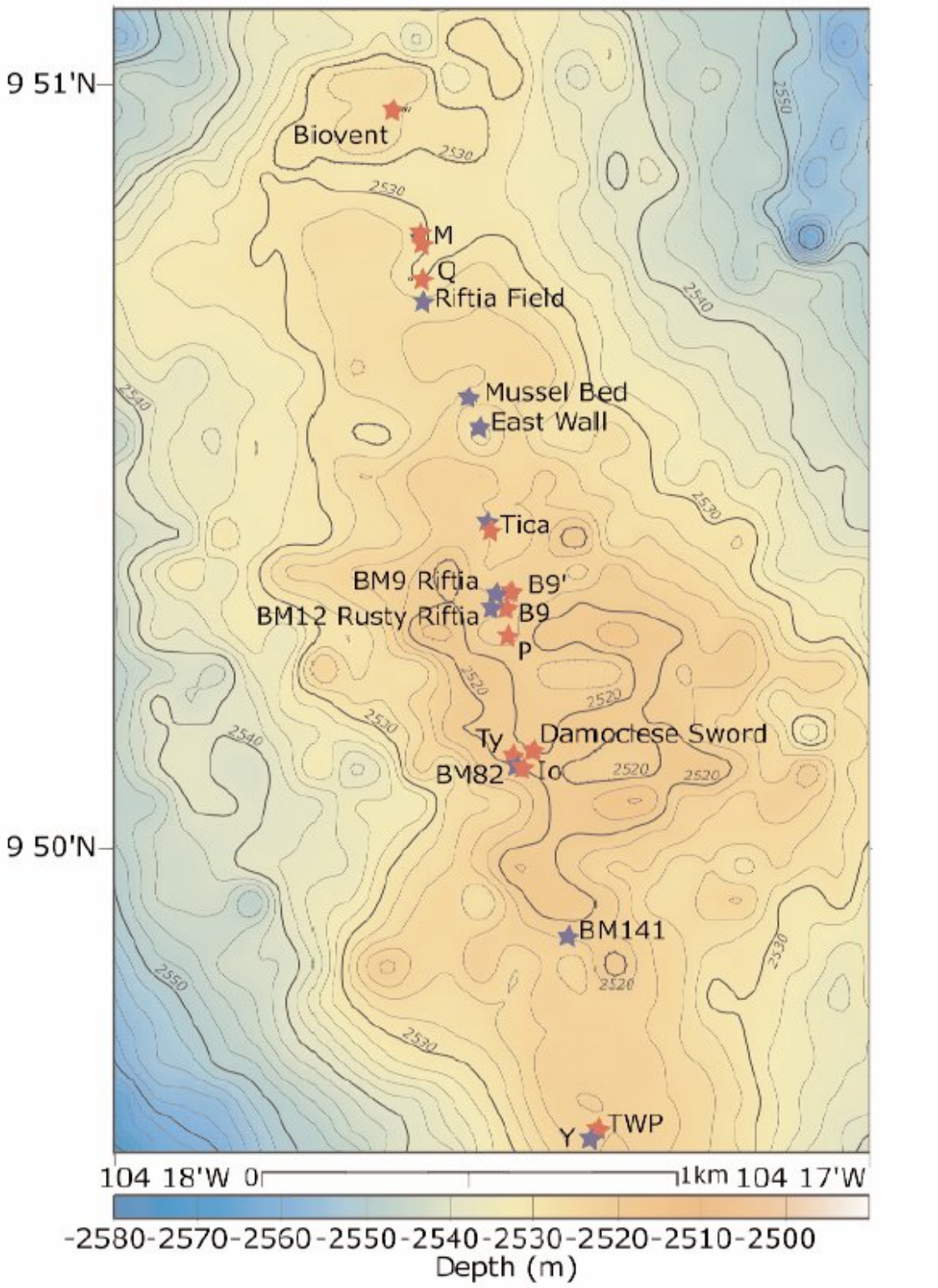

Figure 2.1: Location of the vent field sites at 9°50'N, EPR. [from *Fornari et al., 2004*]

To study the evolution of the vent fluid over time, a rate of production of floc for each of the dates is computed discretely then the data is interpolated between each of the discrete dates to obtain a continuous rate of floc creation. For each date, the mixing ratio is determined by using the concentrations of Si in the high temperature fluid, diffuse flow fluid and seawater, assuming the diffuse flow fluid is simply a mixture of high temperature fluid and seawater. Si, Mg and Cl were all investigated as possible mixing ratio sources but Si consistently gave mixing ratios between 5 and 10 percent, which is why it was chosen for the mixing ratio. A key assumption here is that the diffuse fluid is a very well mixed combination of high temperature fluid and seawater. Without this assumption, it is impossible to conclude anything about the chemical data when it comes to utilization rates. Assuming that the diffuse flow fluid is a mixture of the high temperature fluid and ordinary seawater, as shown schematically in Figure 2.2, the mass flow rate of fluid into the system from seawater (Q_{water}) and high temperature fluid (Q_{high}) is equal to the mass flow rate of fluid out of the system ($Q_{diffuse}$).

$$Q_{water} + Q_{high} = Q_{diffuse} \tag{2.1}$$

Similarly, conservation of Si requires that

$$Q_{water} Si_{water} + Q_{high} Si_{high} = Q_{diffuse} Si_{diffuse} \tag{2.2}$$

Since Si is a passive tracer, it will have no source or sink term in the mass balance equation. From Equations 2.1 and 2.2 the mixing ratio is

$$x = \frac{Si_{diffuse} - Si_{water}}{Si_{high} - Si_{water}} \tag{2.3}$$

The mixing ratio is then used to find how much H_2S is being utilized by the bacteria as well as how much is being converted into pyrite (FeS_2). Equation 2.4 shows how the hydrogen sulfide sink is calculated. Equation 2.4 is simply found by using Equations 2.1 and 2.2 with a sink term in them

$$H_2S_{sink} = xH_2S_{high} + (1-x)H_2S_{water} - H_2S_{diffuse} \tag{2.4}$$

Iron being converted into pyrite will cause the H_2S sink to be diminished. The H_2S sink can be adjusted by applying Equation 2.4 to iron, then subtracting off the amount of H_2S that would go to pyrite creation, which is associated with the iron sink. The mixing ratio of high temperature fluid in diffuse flow fluid is denoted by *x*; therefore the mixing ratio of normal seawater in the diffuse flow fluid is (1-*x*). The mixing ratio, *x*, is found by using Si values in the vent fluids. After the iron adjustments, the sink of H_2S is assumed to be completely used by the biota. This is a reasonable assumption because the effect of iron has already been considered, and iron is the primary reactant with the sulfide. There is the possibility that there are stores of H_2S beneath the seafloor, but these would probably not be long lived and therefore the amount of H_2S consumed by the bacteria is at most the amount of H_2S from the sink.

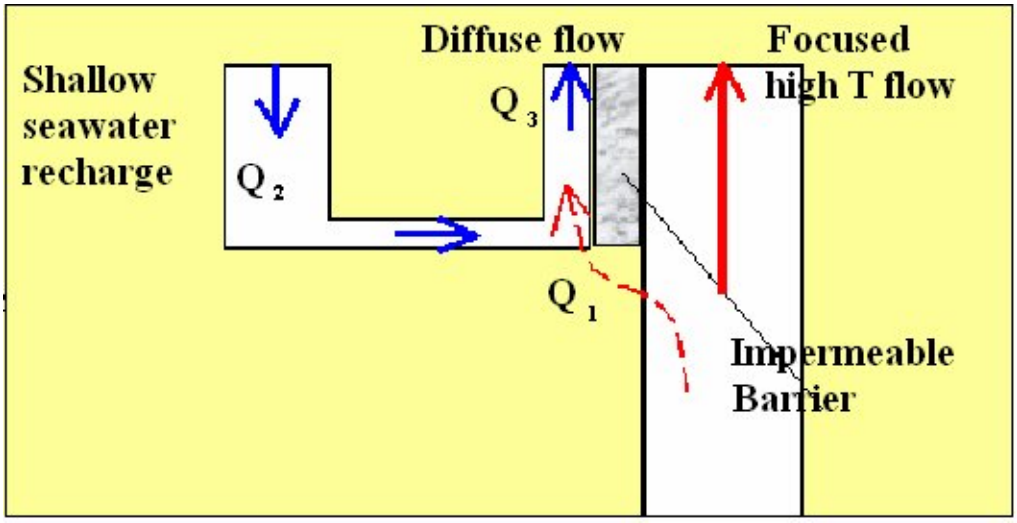

Figure 2.2: Diagram of the creation of diffuse flow fluids by mixing a small amount of high temperature fluid with ordinary seawater [adapted from *Lowell et al.*, 2003].

The basic chemical reaction the bacteria utilize to create the elemental sulfur is listed in Equation 2.5 [*Kelley et al*., 2002].

$$CO_2 + O_2 + 4[H_2S] \leftrightarrow CH_2O + 4[S] + 3[H_2O] \qquad (2.5)$$

To obtain the mass flow rate of H_2S per unit area of seafloor through the system, the following expression is used, with m_{H_2S}, u, φ, ρ_f and $(H_2S_{sink})_{Feadjusted}$ being the molar mass of hydrogen sulfide, Darcian velocity, porosity of the system, density of water, and the iron adjusted sink concentration of H_2S respectively:

$$q_{H_2S} = \frac{u(H_2S_{sink})_{Feadjusted}\,\rho_f\, m_{H_2S}}{\phi} \qquad (2.6)$$

The Darcian velocity is calculated through a vertical boundary layer problem of constant temperature at 100 ^{o}C [*Bejan*, 1995]. Figure 2.3 shows how the temperature and velocity profiles near a vertical temperature boundary change as one approaches the boundary layer. The boundary layer, δ, is related to the height of the vertical boundary, *y,* by the following scaling law, where Ra is the Rayleigh number for the system [*Bejan*, 1995].

$$\frac{\delta}{y} \sim Ra_y^{-1/2} \tag{2.7}$$

$$Ra_y = \frac{kg\beta y \Delta T}{a\upsilon} \tag{2.8}$$

In Equation 2.8, k is permeability, g is the acceleration due to gravity, β is the coefficient of thermal expansion, y is the vertical boundary height, ΔT is the difference in temperature between the wall and the far-field, a is the thermal diffusivity and υ is the kinematic viscosity of the fluid. Assuming that the vertical boundary layer, y, of 100 ^{o}C is 1 km in height, then given a range of permeability from 10^{-11} to 10^{-13} m^2, the boundary layer thickness will be from 3 meters wide up to 30 meters. The uppermost 200 meters of basaltic ocean crust is characterized by high permeabilities between 10^{-12} and 10^{-15} m^2 [*Fisher*, 1998]. This shows that over the given area, the Darcian velocity can be assumed by the vertical boundary problem. The Darcian velocity is calculated by using the following scaling relationship

$$u \sim \frac{a}{y} Ra_y \tag{2.9}$$

To relate the mass flow rate of H_2S to the mass creation rate of floc, all that is needed is the ratio of the molar masses of H_2S to S and the fact that 75% of the floc is elemental sulfur.

$$q_{floc} = \frac{64}{51} q_{H_2S} \tag{2.10}$$

Knowing that 75% of the floc is elemental sulfur, the molar mass ratio of elemental sulfur to Hydrogen Sulfide is 32/34 and the molar ratio of H_2S to S is 1 to 1, as seen in Equation 2.5, derives the factor of 64/51 in Equation 2.7.

The volume of floc created under a given area of seafloor, which is defined as the horizontal boundary layer, δ, multiplied by the length of ridge axis, l_{ridge}, in a set amount of time, t, is

$$\frac{V_{floc}}{l_{ridge}} = 2\frac{q_{floc} t \delta}{\rho_{floc}} \tag{2.11}$$

To find the volume of floc created in between two time intervals of the EPR chemical data [*Von Damm and Lilley*, 2004], the average sink of H_2S is used between the two points to find q_{floc}. The value of t is given by the time between the data points. The volume of floc created at the Northern and Southern Transects of the EPR per km of ridge axis can be seen in Figure 2.4 for a range of Darcian velocities corresponding to permeability values between 10^{-11} and 10^{-13} m^2.

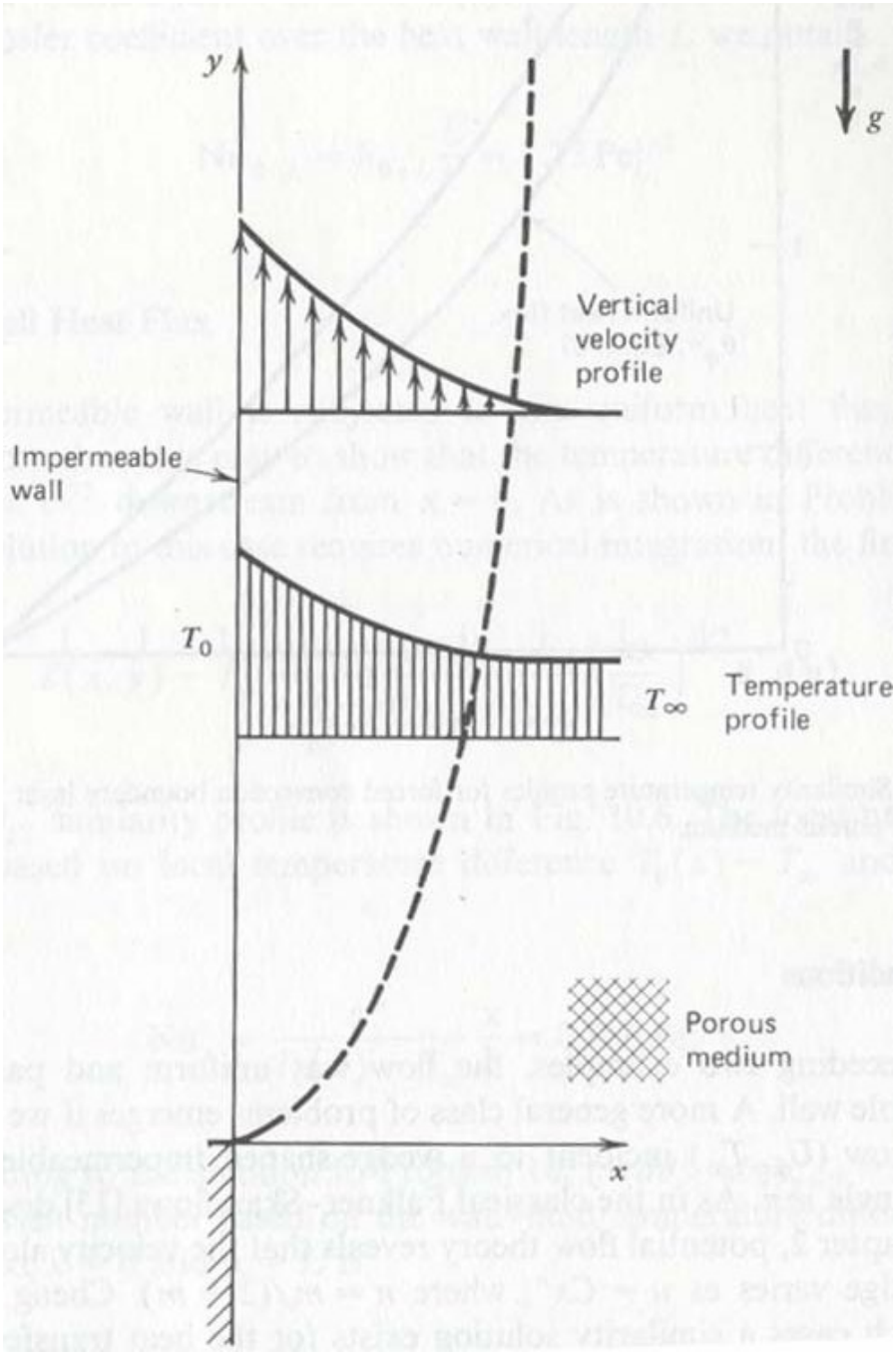

Figure 2.3: Natural convection boundary layer through a porous medium near a vertically heated wall [from *Bejan*, 1995]

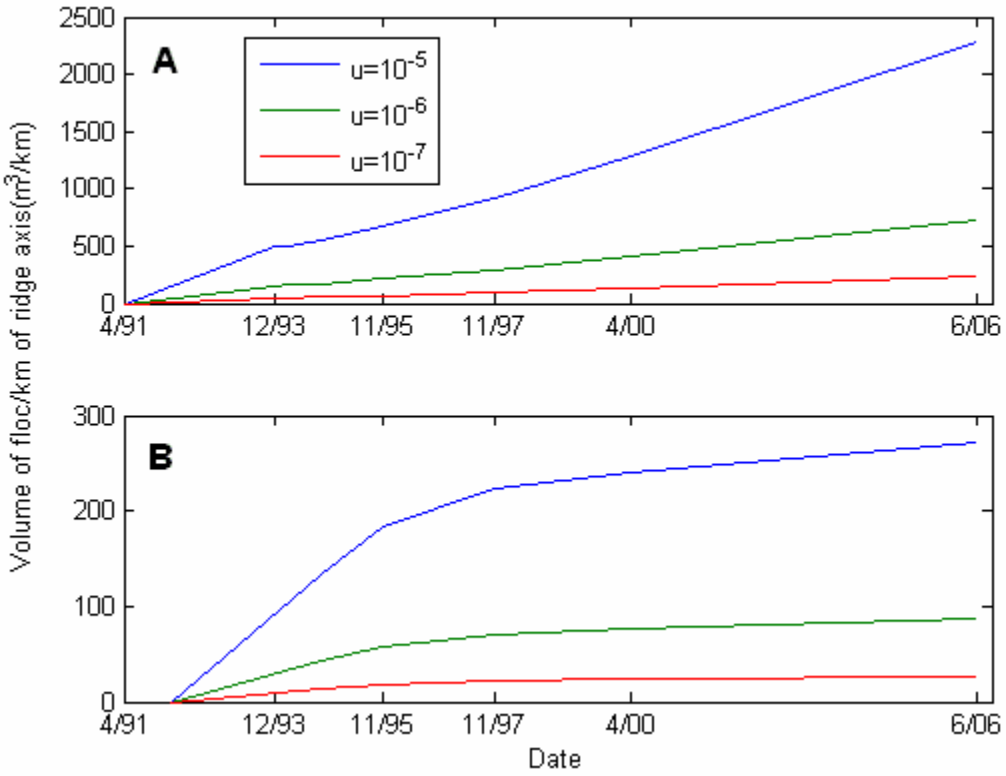

Figure 2.4: Volume of Sulfur floc created at the (**A**) Northern Transect and (**B**) Southern Transect of the EPR per km of ridge axis using chemical data from 1991 to 2000 [*Von Damm and Lilley*, 2004]. Data is extrapolated from April, 2000 to June, 2006. Darcian velocity, *u*, is in m/s.

2.2.2: Maximum Floc Production

To obtain an upper limit on filamentous sulfur production, it is necessary to get a good estimate on the population size of thermophiles in this environment. In 18°C fluids, the numbers of thermophiles in the floc regions of the Co-Axial Segment on the JDF Ridge are on the order of 10^8 bacteria per liter of seawater [*Holden et al*., 1998]. To get the total amount of floc created, a maximum growth rate of 3 μm/min along with a radius of 1.0 μm for the cylindrical filamentous

sulfur [*Taylor and Wirsen*, 1997]. The volume of floc being produced in 1 liter of seawater per minute is estimated by the following relationship:

$$\frac{V_{floc}}{l_{ridge}} = 2\pi r_{floc}^{\ 2} B X_{floc} u t^2 \delta \qquad (2.12)$$

V_{floc} is the volume of floc being produced per liter of seawater, t is time in minutes, X_{floc} is the maximum growth rate of the floc, r_{floc} is the radius of the floc cylinders and B is the bacteria count per unit volume of water. The factor of 2 comes from the symmetry of the system, in that floc will be created on both sides of the axis.

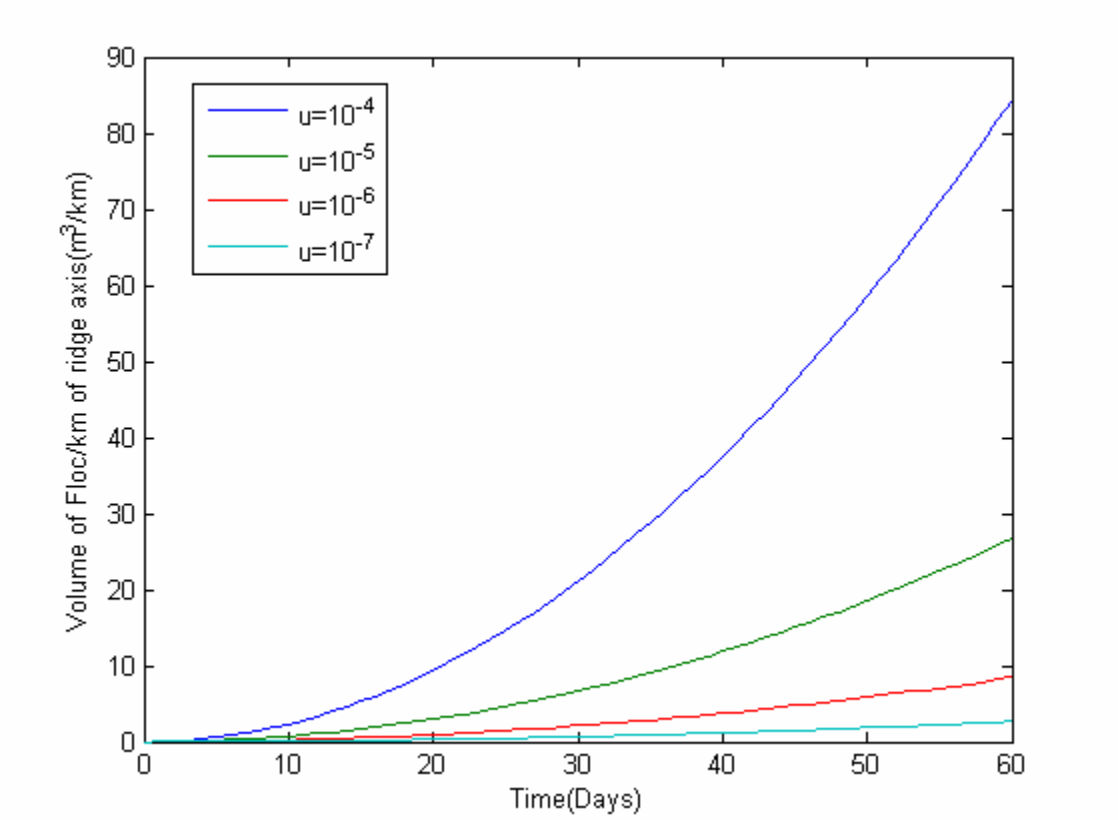

Figure 2.5: The volume of floc created under optimal conditions using the maximum model given a range of Darcian velocities for the region.

Using the aforementioned data, the total volume of floc being created per km of ridge axis can be seen in Figure 2.5 with respect to a range of Darcian velocities that correspond to permeabilities between 10^{-10} and 10^{-13} m^2. With each change in permeability, there is also a corresponding change in boundary layer thickness, which is taken into account in Equation 2.12. This creation rate of floc follows the assumption that the number of bacteria per unit volume stays constant.

2.3: Discussion

2.3.1: Theoretical Porosity Change due to Floc Production

A fundamental question that arises from the modeling of filamentous sulfur production is whether or not it will have an effect on the fluid flow by changing the porosity of the rock. The values for the key parameters will be as follows: $\varphi = 0.1$, l_{ridge}=1000 m, ρ_{floc} = 2000 kg/m3 and d = 10 m, where φ is the porosity, l_{ridge} is the length of ridge axis and d is the depth of the rock. The depth of the rock is simply an assumption because there is some uncertainty as to the real depth of the subsurface biosphere, but it is believed to be small for this case since oxygen is important to the oxidation of sulfide into elemental sulfur. The total volume of the pore space will be:

$$V_{pore} = \varphi l_{ridge} d\delta \qquad (2.13)$$

Using the maximum floc production model with the volume of the pores equal to the volume of the floc produced, the time to fill all of the pore space can be obtained. Using the maximum floc creation rate, it would take around 25 years to fill all of the pore space in the diffuse flow area if the Darcian velocity is 10^{-7} m/s, 8 years with a Darcian velocity of 10^{-6} m/s, 3 years with a Darican velocity of 10^{-5} m/s and 300 days with a Darcian velocity of 10^{-4} m/s, assuming constant maximum growth rate.

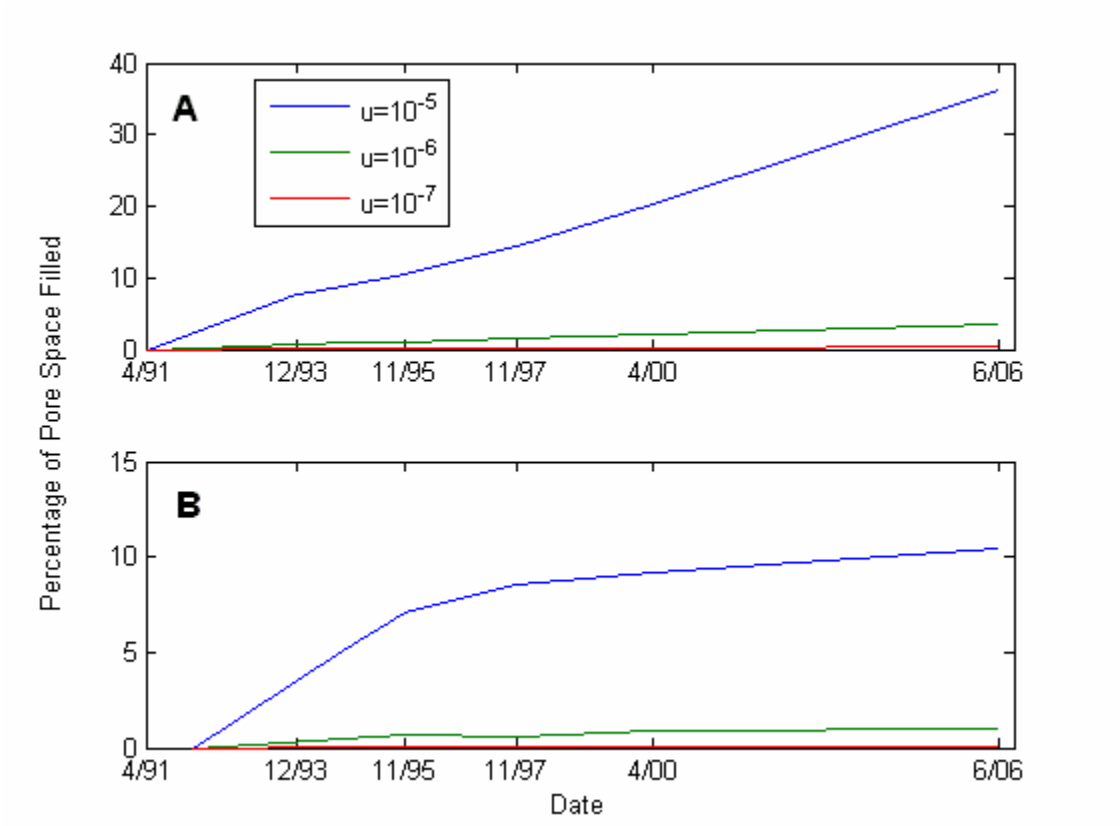

Figure 2.6: Percentage of pore space occupied by sulfur floc since 1991 eruption. Data from the Northern (**A**) and Southern (**B**) Transects [*Von Damm and Lilley*, 2004] are used to calculate the volume of floc produced per km of ridge axis. Data is extrapolated from April 2000 to June 2006.

Using the chemical data, a piecewise function of porosity change over the ten year period after the 1991 eruption is developed. By applying these data in conjunction with a Darcian velocity of 10^{-5} m/s, one would expect 9% and 20% of the pore space at the Southern and

Northern transects, respectively, to be filled with sulfur floc by April, 2000 (Figure 2.6). As the Darcian velocity decreases by an order of magnitude, the percent of pore space filled with floc will decrease by an order of magnitude. If porosity were reduced by 20% and the permeability followed a Carmen-Kozeny type relationship $k \propto \phi^3$, the permeability would be reduced by a factor of 2. This is not a significant factor, so one would not expect a large scale change in the fluid dynamics of the hydrothermal system given the amount of floc that is being produced.

2.3.2: Comparison of Observed Floc Production with Both Models

Observations from the 'snowblower' event of 1991 on the EPR indicate a highly porous floc being emitted and being deposited an average of 5 cm thick on the seafloor up to a distance of 100 meters from the ridge axis [*Haymon et al*., 1993; *Taylor and Wirsen*, 1997]. If a uniform thickness of 5 cm and uniform porosity of 0.9 for the floc is assumed, a rough estimate of how much floc was emitted per km of ridge axis can be obtained. Taking 100 meters from each side of the ridge axis and 1 km of ridge to be the area, 1000 m^3 of floc per km of ridge would be created.

For the maximum production of floc, it would take around 210 days to create the amount of floc being seen on the seafloor during an eruption for a Darcian velocity of 10^{-4} m/s. Using the chemical data from the Northern Transect, the estimated floc produced in the 1991 eruption would be accomplished by 1998 given a Darcian velocity of 10^{-5} m/s years (see Figure 2.4a). Using the chemical data from the Southern Transect, however, only about 25% of the estimated floc production would have occurred by the year 2000, even with the highest flow rates used (see Figure 2.4b).

From the observed floc production at the 1991 ‘snowblower’ event, it would take a very high flow rate to create the amount of floc observed with the maximum production model. This means that it is more probable that the floc observed in a ‘snowblower’ event is stored in residence over a long period of time instead of being created during an eruption type event. A sizeable portion of the observed floc should be stored in residence according to the chemical model, and as long as it is easily flushed out during an eruption, this is very likely to be the case.

2.4: Conclusions

The way ‘snowblower’ events are created is most likely caused by an eruption event in which a large amount of hydrogen sulfide and other nutrients are introduced into the biosphere, but the results are still inconclusive. It is entirely possible for a vent community to create the observed floc at a slow rate over a few decades time since the recurrence of eruption events is many years. The use of radioisotopes could help shed some light on ‘snowblower’ events, but the number of observed events is too few to have any conclusive evidence. The metabolism of elemental sulfur by other microbes is not taken into account in any of the models, and this mechanism could prevent any sulfur from being stored in residence for long periods of time. The quasi steady state model for floc production could be off by an order of magnitude due to an uncertainty in the flow speed through the system since the flow speed was calculated using a theoretical vertical temperature boundary and some of the parameters involved in the calculation such as permeability can easily be off by an order of magnitude. Also, the horizontal distance from the vertical temperature barrier will affect the flow speed up to a factor of 4. Recent studies [*Ramondenc et al*., 2006] have started to measure flow speeds in the diffuse flow regions of

hydrothermal vents, but nutrient fluxes can vary throughout the system due to horizontal and vertical mixing.

The effect of filamentous sulfur on porosity is small, and under the most ideal conditions, porosity would be relatively constant. In the optimal floc creation criteria, porosity would take many years to be completely filled up, depending on the flow rates. In the time between eruptions using the chemical data, the porosity will probably be changed by less than 10 percent over 10 years. Given a Darcian velocity of 10^{-6} m/s, only 2% of the pore space will be filled after 10 years.

The recent 2005 'snowblower' event on the EPR 9^{o}N site has indicated that much less floc than that for the 1991 event has been seen. This may indicate that all of the floc emitted during the recent eruption was stored in residence because according to the chemical data, one would expect to see less floc than the 1991 event. This may also indicate that there was a much larger time frame between the 1991 eruption and the one previous to that, and floc may always be stored in residence.

CHAPTER 3

SULFATE REDUCTION

3.1: Introduction

Along continental margins, the metabolic process of sulfate reduction is responsible for about 50% of all the carbon oxidized in the marine sediments [*Canfield and Des Marais*, 1991]. Sulfate reduction has proven to be incredibly vital in the creation of H_2S, one of the most important processes for sedimentary ecosystems as well as deep-sea hydrothermal vent ecosystems because of the role H_2S plays in maintaining the complex symbioses between animals and microorganisms [*Jorgensen*, 1982]. The reduction of sulfate is been shown to be strongly coupled with the availability of metabolizable organic matter [*Bottcher et al.*, 2004]. Sulfate reducing bacteria have been found in lakes, such as Lake Tanganyika in Africa [*Elsgaard et al.*, 1994] and Lake Mendota in Wisconsin [*Ingvorsen et al.*, 1981], underground mines in Japan [*Kaksonen et al.*, 2006], deep sediments in the southwest Pacific [*Bottcher et al.*, 2004], coastal sediments [*Jorgensen and Bak*, 1991], Arctic sediments [*Knoblauch and Jorgensen*, 1999], and at almost all deep-sea hydrothermal systems.

Sulfate reduction rates as high as 6×10^{-3} mol SO_4/m^3day have been found in continental margin marine sediments [*Canfield and Des Marais*, 1991], and sulfate reduction rates in hydrothermal vent systems with large amounts of sediments such as Guaymas Basin have been found to be even larger than this [*Jorgensen et al.*, 1992]. *Kallmeyer and Boetius* [2004] found sulfate reduction rates at Guaymas Basin to be several moles per cubic meter per day. Ordinary

deep-sea hydrothermal systems tend to have sulfate reduction rates many orders of magnitude than in sedimentary environments. Figure 3.1 illustrates this fact by showing the rate of sulfate reduction for different sedimentary marine environments.

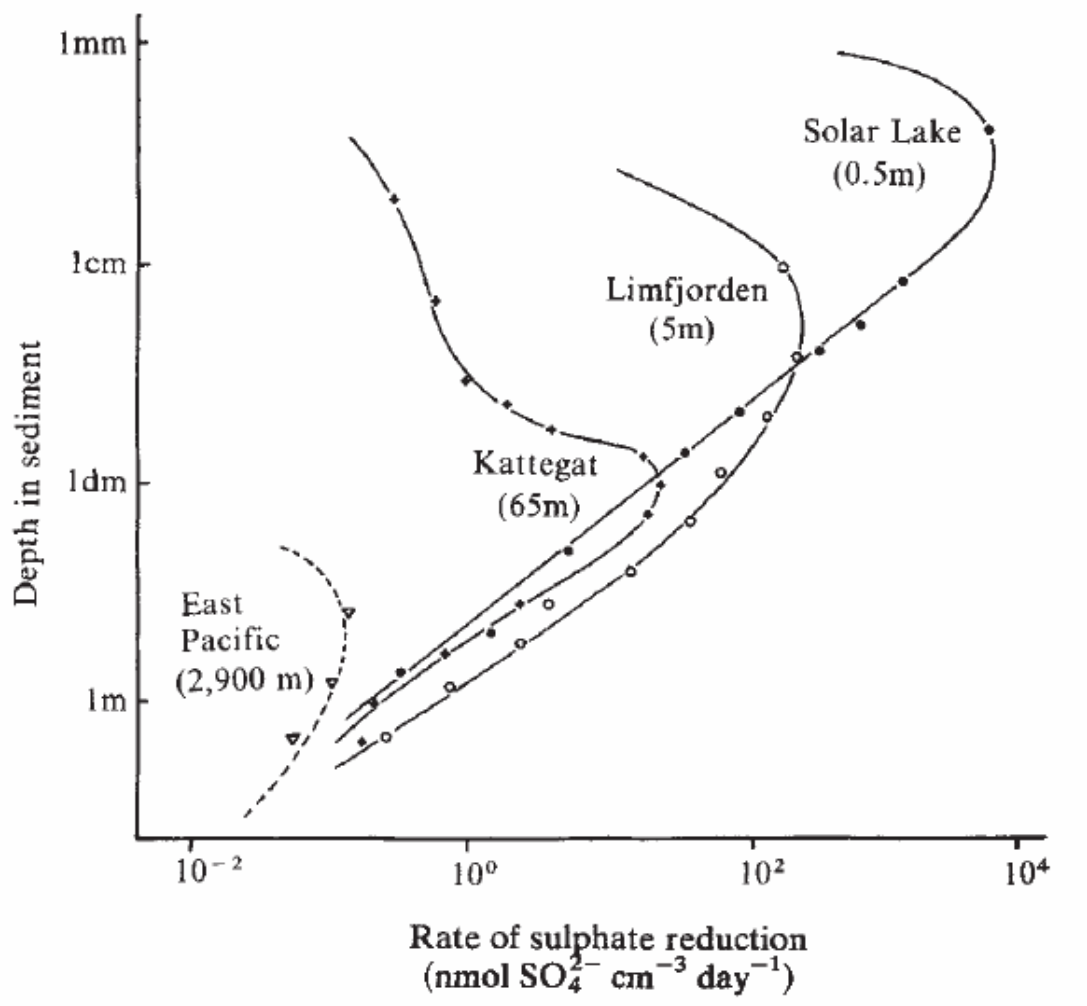

Figure 3.1: Rate of bacterial sulfate reduction for various sedimentary regimes [from *Jorgensen*, 1982].

At mid-ocean ridge hydrothermal systems, the precipitation of anhydrite from seawater sulfate during recharge has direct implications on the overall porosity and permeability structure of the system. Circulating seawater is expected to lose some or its entire load of sulfate due to

the precipitation of anhydrite during the heating of seawater above 130 ^{o}C [*Jannasch and Mottl*, 1985; *Lowell and Yao*, 2002]. Anhydrite precipitation has direct implications toward biogenic sulfate reduction. If biogenic sulfate reduction is large, there will be less sulfate that can precipitate as anhydrite. If biogenic sulfate reduction is small, more sulfate can precipitate as anhydrite, potentially sealing pore space in the process.

In this chapter, a model for the production of biogenic sulfate reduction is presented and is used to create concentration profiles as a function of depth for various flow speeds in the recharge regions of deep-sea hydrothermal systems. The model is created by using sulfate reduction rate curves from the Guaymas Basin in Mexico [*Jorgensen et al.*, 1992], a steady state 1-D advection-diffusion temperature equation, and a 1-D, steady-state, advection dominated conservation of solute equation. This model is then compared with a model that utilizes Gibbs free energy to quantify biogenic sulfate reduction [*Bach and Edwards*, 2003]. This comparison shows that the data from *Jorgensen et al.* [1992] cannot be applied directly to hydrothermal recharge zones at mid-ocean ridges. At the high rates determined by *Jorgensen et al.* [1992], biological activity would reduce all seawater sulfate transported into the system within the upper 10 meters or less of the crust. The diffusivity of sulfate in seawater is on the order of $\sim 10^{-10}$ m^2/s, and it is shown that unless the flow speeds are incredibly low ($<10^{-12}$ m/s), the effects of diffusion are negligible, except within thin diffusive boundary layers. Finally, the effect of anhydrite precipitation is briefly overviewed and it is found that anhydrite precipitation has little to no effect on porosity because the time it would take to seal pore space would be on the order of thousands of years provided the flow speeds are $\leq 10^{-9}$ m/s. At these slower flow speeds, the effects of biogenic sulfate reduction are greater and it would take even longer for anhydrite precipitation to seal pore space.

3.2: Model

To create the model for bacterial sulfate reduction at mid-ocean ridge recharge zones, it is necessary to have a depth dependant temperature profile and a temperature dependant sulfate reduction profile. For the depth dependant temperature profile, I consider a 1-D steady state heat transfer problem with uniform velocity in the z-direction and no sources. The associated conservation equation in a porous medium is

$$\rho_f c_f \phi v_z \frac{dT}{dz} = \lambda_m \frac{d^2T}{dz^2} \tag{3.1}$$

By factoring out one of the differentials and setting $a=\lambda_m/\rho_f c_f$, Equation 3.1 becomes

$$\frac{d}{dz}\left(\frac{dT}{dz} - \frac{\phi v_z}{a} T\right) = 0 \tag{3.2}$$

The general solution to Equation 3.2 is of the form

$$Ae^{-\phi v_z z/a} + B = T \tag{3.3}$$

By applying a boundary condition of $T = 0$ at the surface ($z = 0$) and $T = T_o$ at the bottom of the system ($z = H$), the following solution is obtained for the temperature profile

$$T = T_o \frac{(e^{-\phi v_z z / a} - 1)}{(e^{-\phi v_z H / a} - 1)} \tag{3.4}$$

Figure 3.2 shows the temperature profile for various values of v_z. The temperature profile in Equation 3.4 needs to be coupled to a chemical transport equation through the temperature dependant sulfate reduction equation. The chemical transport equation is [*Phillips*, 1991]

$$\frac{\partial C_i}{\partial t} + \nabla \cdot (v_z C_i) = \nabla \cdot D_p \nabla C_i + Q_c \tag{3.5}$$

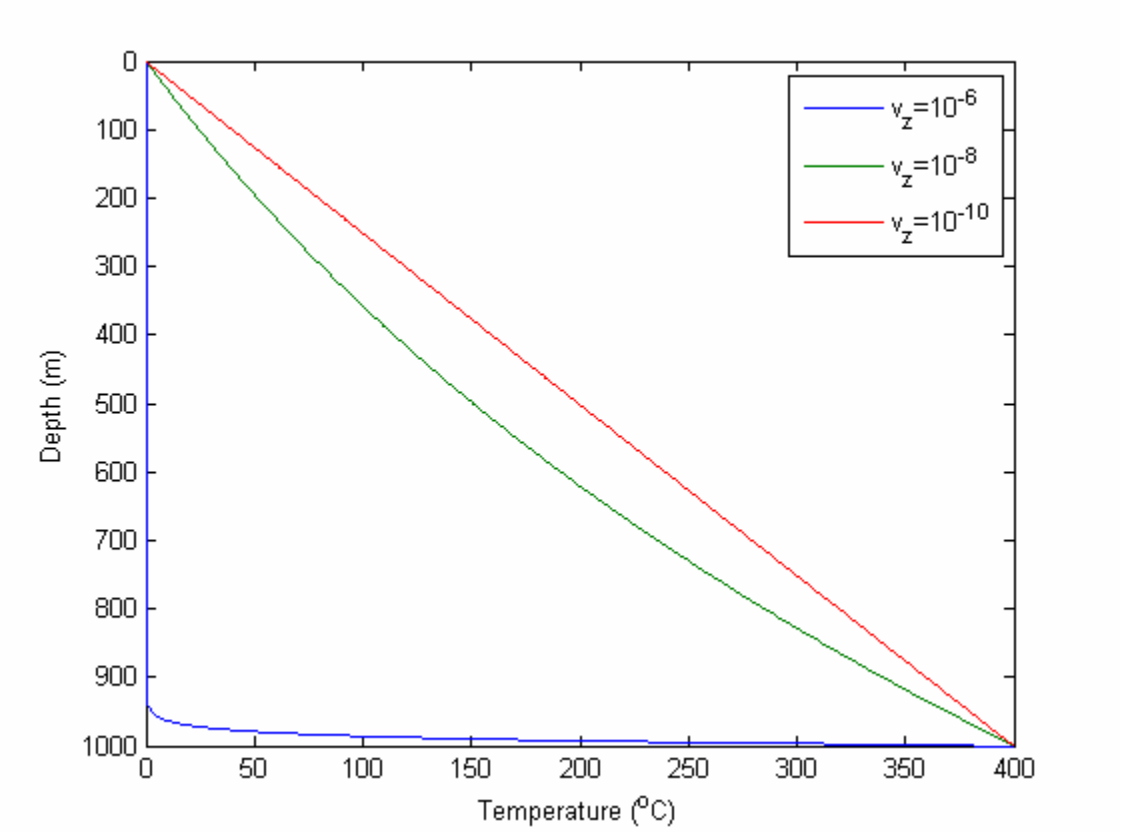

Figure 3.2: Theoretical temperature profiles for various flow rates, given in m/s, with porosity, ϕ = 10%.

It can be assumed that the chemical transport will be steady state because there is a constant flux of chemicals at velocity v_z into the system from the top. It is also appropriate to assume that chemical diffusion will be negligible over most of the flow path because the diffusion term on the right hand side of Equation 3.5 is many orders of magnitude smaller than the advection term on the left hand side of the equation. Equation 3.5 in 1-D then reduces to

$$v_z \frac{\partial C_i}{\partial z} = Q_c \tag{3.6}$$

Using sulfate reduction data (Figure 3.3) obtained from sediment cores taken from the hydrothermal vent field at Guaymas Basin in the Gulf of California spreading center [*Jorgensen et al.*, 1992], a sulfate reduction rate as a function of temperature can be found. This is accomplished by taking sulfate reduction rates for every 10 ^{o}C and each 5 cm interval from each of the curves in Figure 3.3, then averaging the data from each 5 cm interval. The result is shown in Figure 3.4. Note that the data in Figure 3.3 was obtained from a number of 10 mL samples from each 5 cm interval. The data in Figure 3.4 is given as mole/m^{3}s rather than μmol/day, which reflects this volume averaging. A 6th order polynomial is then fit to the data in Figure 3.4. The polynomial is of the form

$$SRR = AT^6 + BT^5 + CT^4 + DT^3 + ET^2 + FT + G \tag{3.7}$$

The polynomial fit to the laboratory data is visually represented in Figure 3.4. In the sulfate reduction rate curve, sulfate reduction above 110 ^{o}C is assumed to be zero because sulfate reducers are not believed to exist above that threshold. Also, the rate at 0 ^{o}C is also set to zero

because seawater in the deep ocean is at 2 ^{o}C, and therefore it is a non-existent solution. The polynomial fitted sulfate reduction rate corresponds directly to the *Qc* term in Equation 3.6.

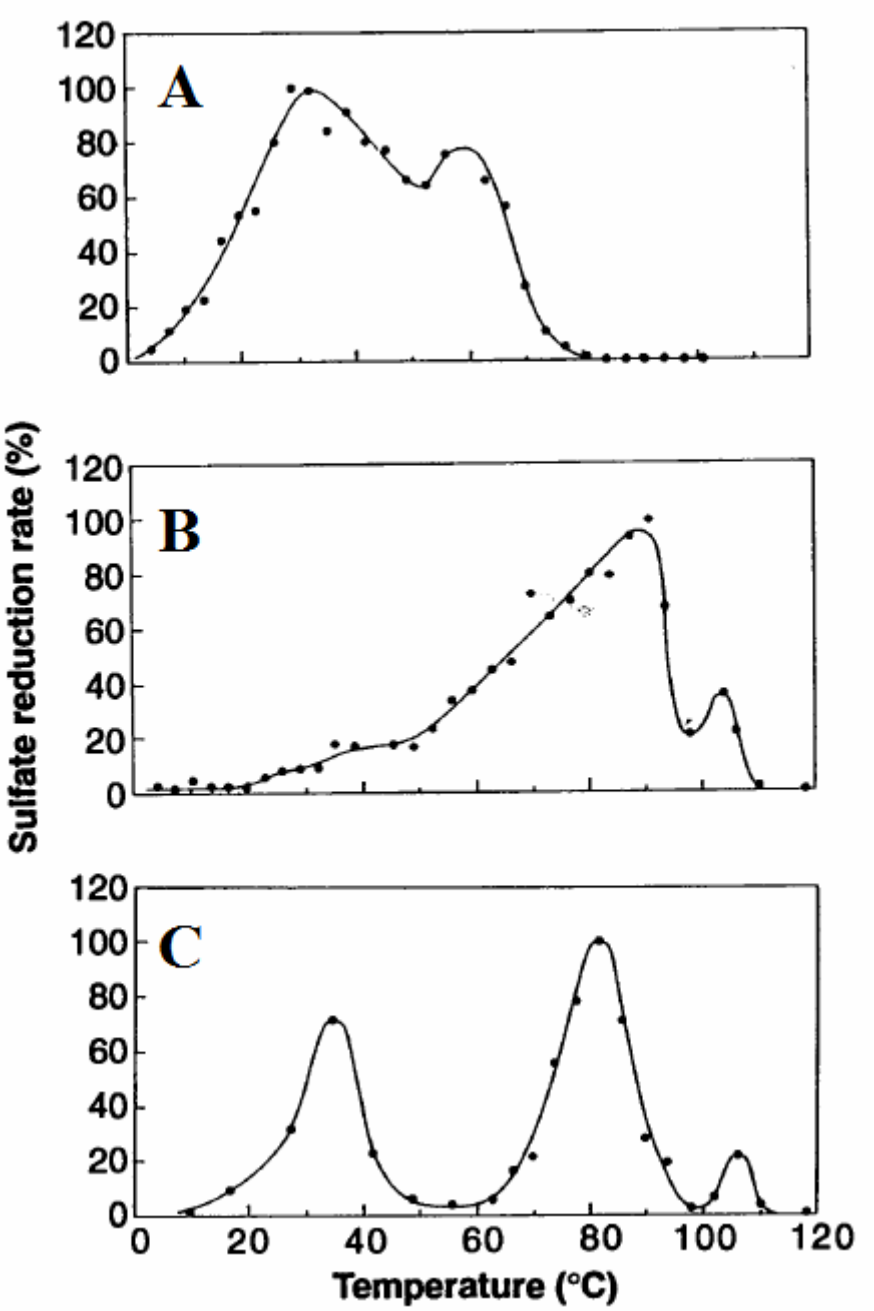

Figure 3.3: Sulfate reduction rate curves as a function of temperature taken from sediment cores from Guaymas Basin, Mexico [from *Jorgensen et al.*, 1992]. The sulfate reduction rate is a percentage of the maximum sulfate reduction rates for the three depths **(A)** 0-5 cm **(B)** 10-15 cm **(C)** 15-20 cm. The maximum sulfate reduction rates are **(A)** 61 µM SO_4/day **(B)** 24 µM SO_4/day **(C)** 19 µM SO_4/day.

The temperature profile of the system (Equation 3.4) is substituted into the sulfate reduction rate curve (Equation 3.7) and then combined with the conservation of solute equation (Equation 3.6) to find out how much solute is consumed per meter at any given point along the vertical profile. Then, the top of the system is given an initial concentration and the sulfate consumption rate is subtracted off of the subsequent control volume's concentration of solute.

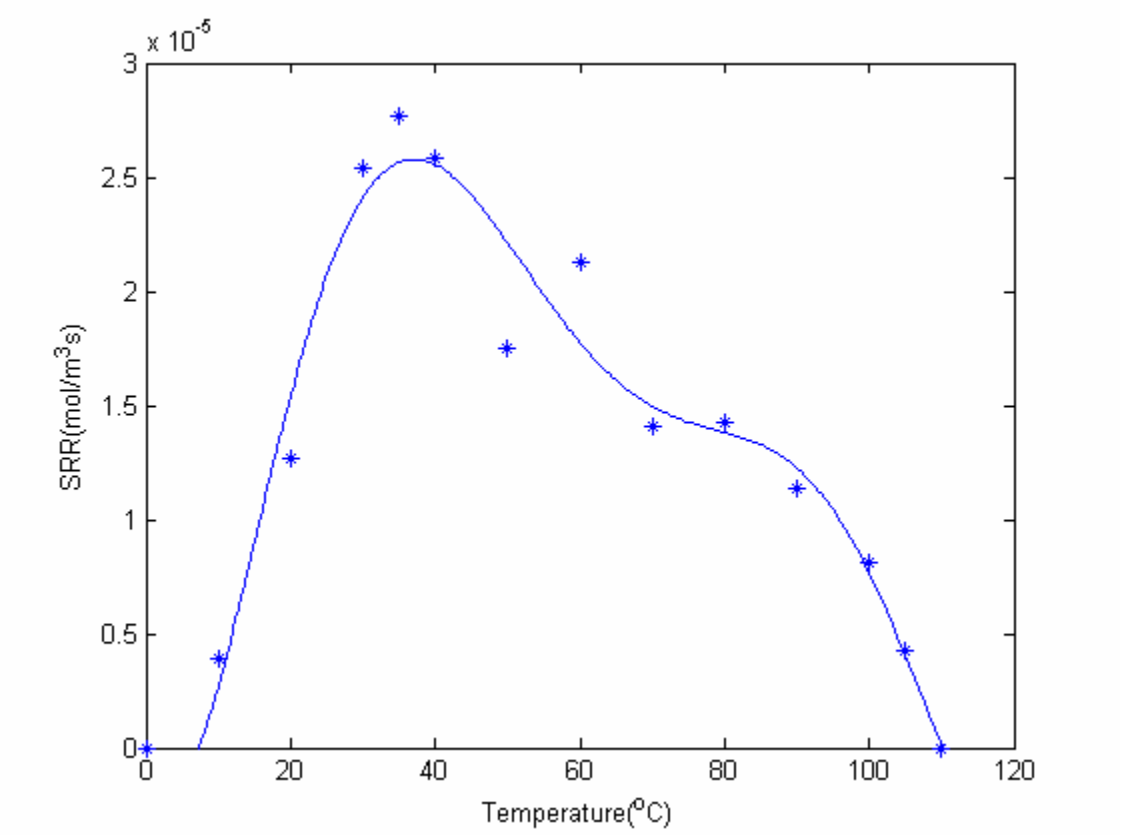

Figure 3.4: Sulfate reduction rate as a function of temperature curve adapted from SRR data from *Jorgensen et al.* [1992].

3.3: Results

3.3.1: Theoretical Model

The data in Figure 3.3 and recast in Figure 3.4 come from a nutrient and sediment rich area within the Guaymas Basin. This area is a poor representation of deep-sea hydrothermal systems, which have almost no sediments, relatively little organic matter, and fluid flow driven by permeable fractures and crevasses, rather than by porous flow through sediments. The data in Figure 3.3 was derived for an upflow environment because the temperature profile, shown in Figure 3.5, goes from 120 ^{o}C at 30 cm depth to 0 ^{o}C at the surface, with a conductive boundary layer over the final 15 cm. The Darcian velocity can be scaled by

$$\delta \sim \frac{a}{u} \tag{3.8}$$

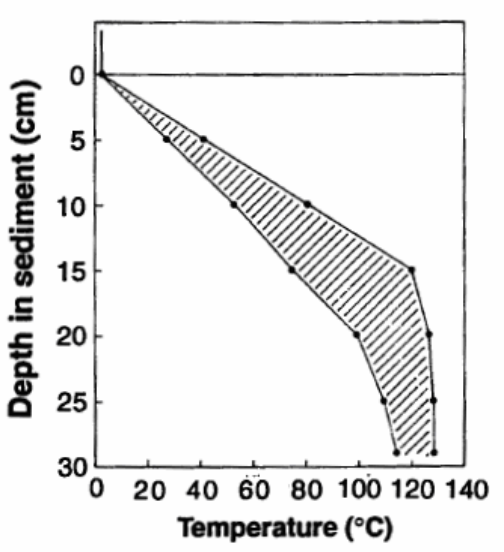

Figure 3.5: Temperature profile for Guaymas Basin sediment cores [from *Jorgensen et al.*, 1992]

For this system, the Darcian velocity would be on the order of ~10^{-5} m/s, and the interstitial velocity would be around ~10^{-4} m/s, given a porosity of 10%. This environment can be modeled using Equations 3.4 and 3.6. The concentration profile as a function of depth is given in Figure 3.6.

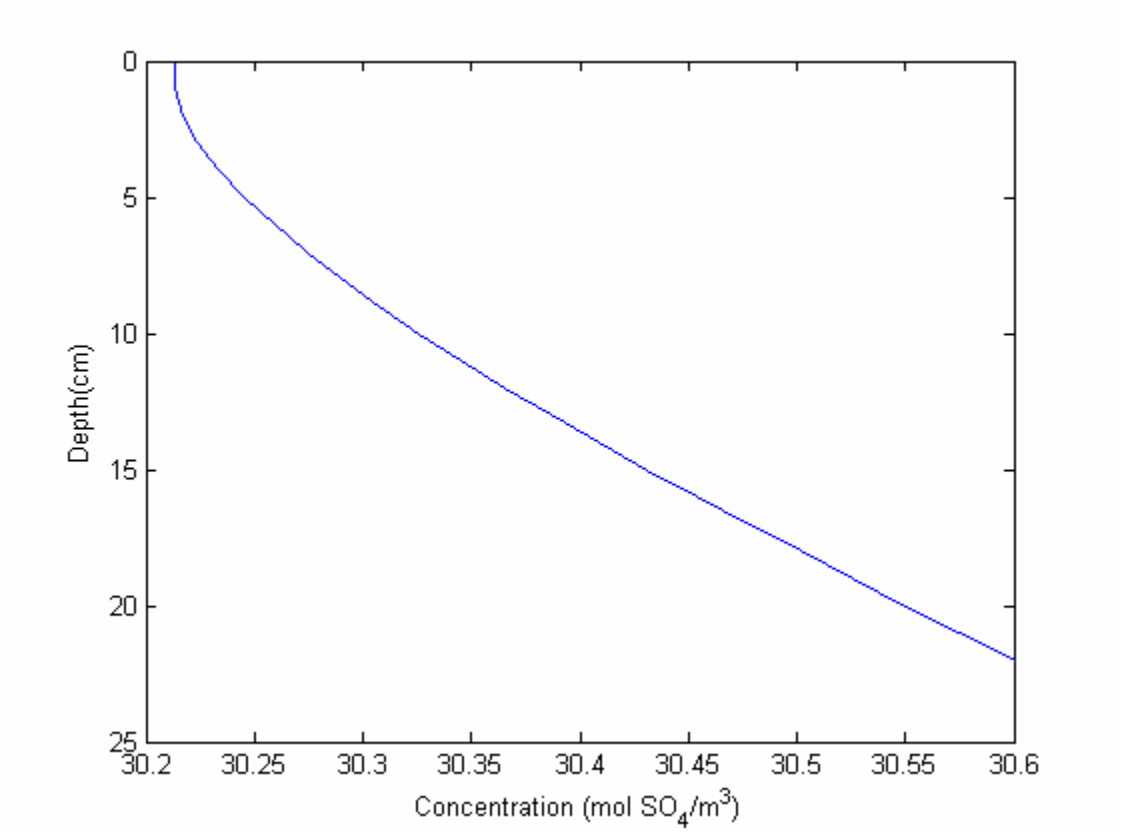

Figure 3.6: Concentration as a function of depth for upflow environment formulated from Guaymas Basin data [*Jorgensen et al.*, 1992]

Figure 3.6 shows that only about one percent of the transported sulfate is reduced by the time it reaches the surface, assuming an advectively dominated system. However, when using slower flow speeds with this theoretical data to model al recharge system in a bare-rock mid-ocean ridge hydrothermal system, biogenic sulfate reduction would appear to remove essentially all the seawater sulfate within the upper tens of meters or less of the crust. A simple scaling

analysis can verify that the Guaymas Basin sulfate reduction rate is too large to be reasonable for a normal recharge zone. The change in concentration scales as

$$\Delta C \sim \frac{(SRR)\Delta z}{v_z} \tag{3.9}$$

From Figure 3.4, an average sulfate reduction rate is 10^{-5} mol SO_4/m^3s. Total removal of sulfate $\Delta C \approx 30$ mol/m^3 would thus occur when the ratio $\Delta z/v_z \geq 3 \times 10^6$ s. For a flow speed of 10^{-5} m/s, the total removal of sulfate would occur within 30 m. For 10^{-10} m/s, the total removal of sulfate would occur within 3×10^{-4} m. When considering a recharge zone at mid-ocean ridges, the flow speed is probably much smaller than an upflow zone and the size is also much larger [*Lowell and Yao*, 2002]. The above result is therefore unrealistic because (a) there is evidence of anhydrite precipitation in the crust [*Alt et al.*, 1986] (b) sulfur isotope data shows that some seawater sulfate appears to be reduced in high temperature basalt seawater reactions [*Seyfried and Bischoff*, 1979; *Seyfried and Mottl*, 1982], and (c) there is evidence of low-temperature basalt seawater reactions that remove sulfate [*Alt et al.*, 1986; *Alt,* 1995].
On the other hand, data from the Ocean Drilling Project (ODP) Leg 64 in the Guaymas Basin show that most seawater sulfate is reduced in the upper hundred meters or so where fluid in flowing downward through the sediments. Site 478, which is located about 12 km northwest of the southern rift segment of the Guaymas Basin, shows seawater sulfate entering the crust and all of it being removed in the upper 100 meters. The temperature profile at Site 478 increases gradually from 2 ^oC at the surface to 30 ^oC at a depth of 500 meters. Site 481 is located very near the hydrothermal site along the northern rift segment of the Guaymas Basin and it exhibits a very similar result in the removal of sulfate. Approximately 80% of the seawater sulfate is

removed within the upper 10 meters. The temperature profile at Site 481 is also very similar to Site 478 except it reaches a temperature of 30 ^{o}C by 400 meters depth. The temperature and sulfate profiles for Sites 478 and 481 are shown in Figure 3.7.

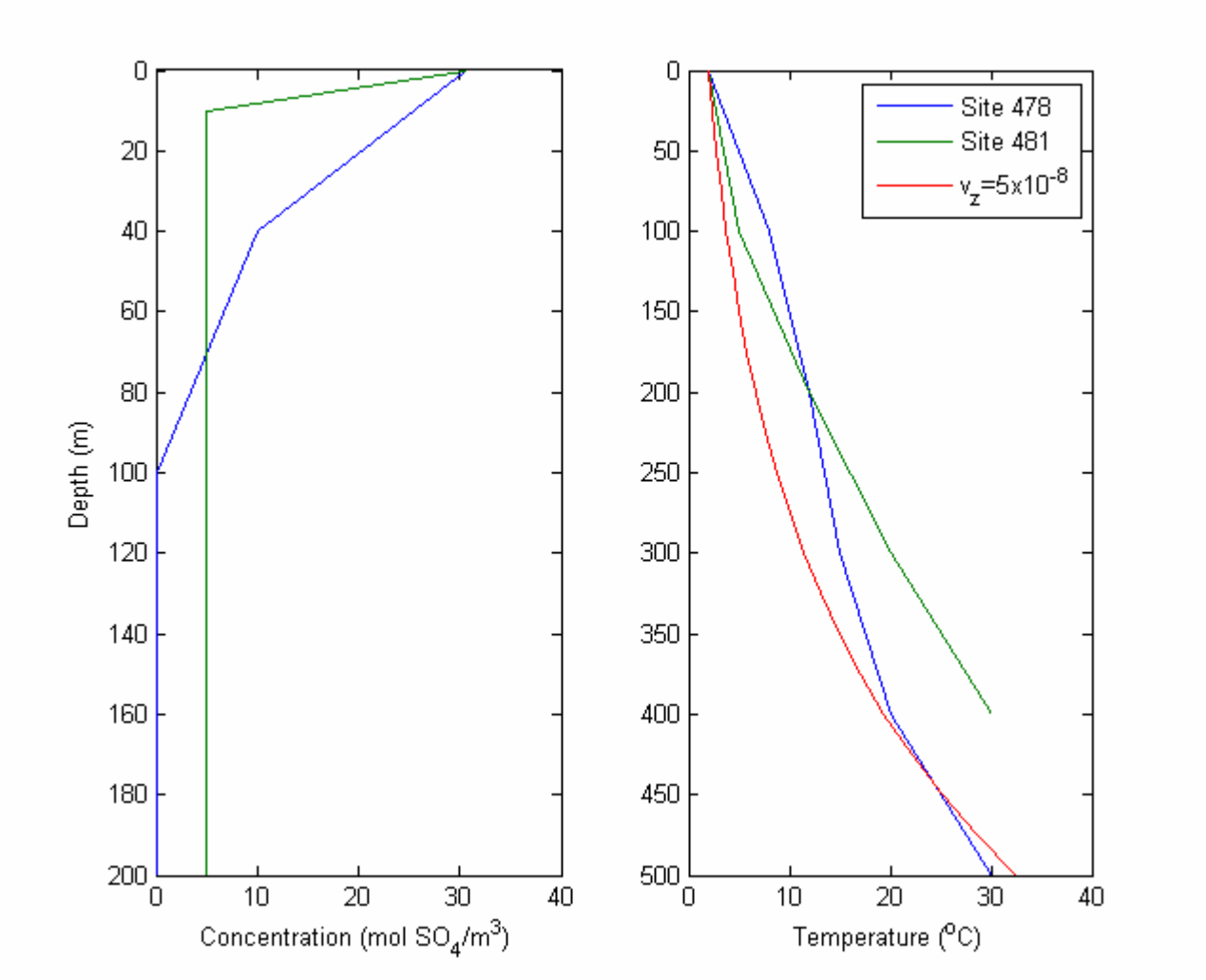

Figure 3.7: Concentration of sulfate and temperature as a function of depth for ODP Leg 64 Sites 478 and 481. The temperature profile for a flow speed of 5 x 10^{-8} m/s through a 10% porous material is plotted in red.

The shape of these temperature profiles is consistent with fluid recharge (see Figure 3.2). The sulfate data from these two sites would indicate that the recharge environment is allowing for the complete removal of seawater sulfate through microorganisms. The temperatures at these

sites are still too low for a significant proportion of the seawater sulfate to be removed through water-rock reactions. The temperature profiles for Sites 478 and 481 indicate a flow speed around ~5 x 10^{-8} m/s. Using the scaling analysis from Equation 3.9 and assuming all of the seawater sulfate is removed by microorganisms, the sulfate reduction rate for Site 478 would be ~10^{-8} mol SO_4/m^3s and ~10^{-7} mol SO_4/m^3s for Site 481. These sulfate reduction rates are still 2 to 3 orders of magnitude less than the sulfate reduction rate obtained from the upflow environment in Figure 3.4.

A study by *Bach and Edwards* [2003] looks at the biogenic sulfate reduction at deep-sea hydrothermal vents worldwide by performing a free energy analysis of sulfate and sulfate transport. They found the overall amount of organic carbon created through sulfate reduction to be 9 ± 7 x 10^{10} gC/yr over all ridge flank segments and a depth z = 500 m, using a Gibbs free energy approach for biogenic pathways. The change in free energy for sulfate is ΔG ~ -22.4 kJ/mol SO_4 [*Sorensen et al.*, 2001] and the Gibbs energy dissipation coefficient is K_G ~ 83 kJ/gC [*Heijnen and Van Dijken*, 1992]. The following expression gives the sulfate reduction rate per unit volume

$$\frac{dC_{SO_4}}{dt} = \frac{(dC_c / dt)K_G}{\Delta GAz} \tag{3.10}$$

When an area of 1.5 x 10^{14} m^2 is utilized for the worldwide ridge flank area [*Bach and Edwards*, 2003], a sulfate reduction rate of 1.3 x 10^{-12} mol SO_4/m^3s is found. The overall transport of sulfate for each m^3 of ridge flank is calculated by taking the seawater sulfate concentration, C_{SO_4} = 30.6 mol/m^3 H_2O, multiplying it by the flow speed, v_z, and dividing by the vertical height of the system, 500 m. Figure 3.8 shows the ratio of sulfate reduction to the sulfate

transport in terms of flow speed. For high flow rates, the amount of sulfate reduced biogenically is almost negligible whereas for slow flow rates, all of the sulfate transported can be reduced. This is directly related to the residence time of the fluid parcel in the system over 1 meter depth. If the flow speed is around 10^{-10} m/s, the residence time will be ~300 years whereas if the flow speed is 10^{-7} m/s, the residence time is on the order of ~4 months.

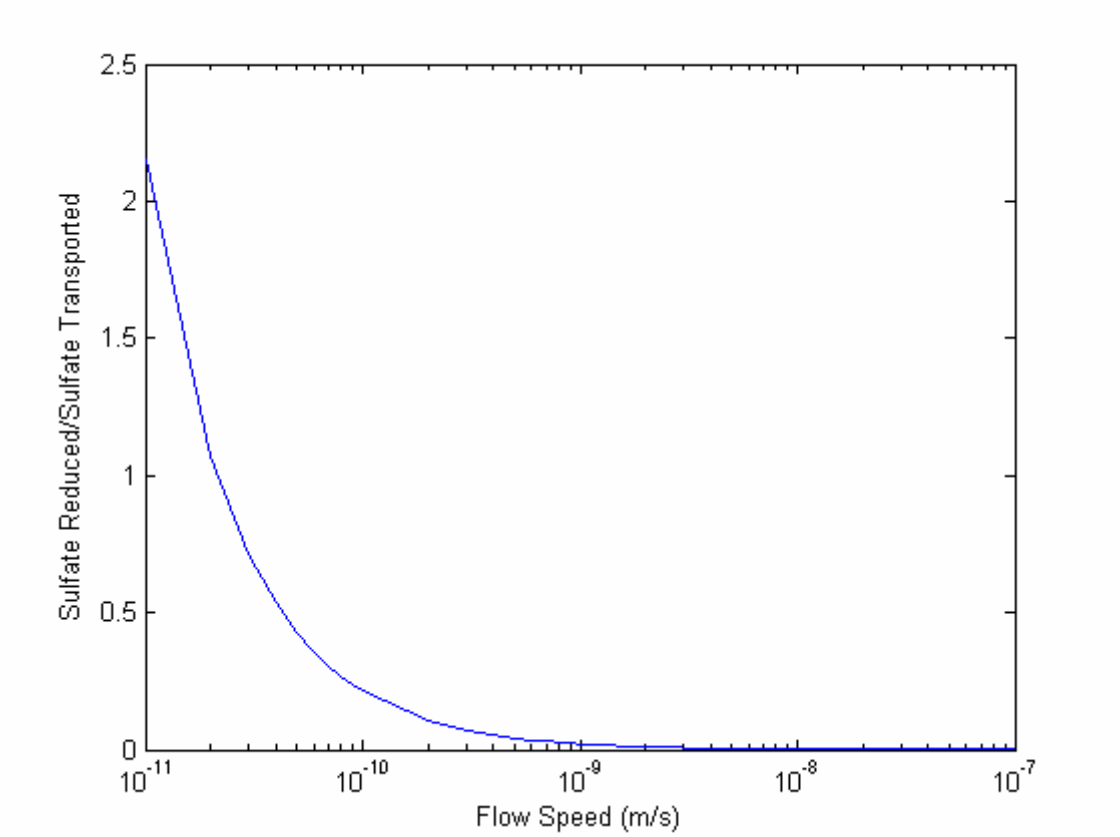

Figure 3.8: Ratio of sulfate reduction in ridge flank segments to the overall sulfate transport over the same area with respect to the flow speed of fluids through the system.

The data from *Bach and Edwards* [2003] can be matched to the theoretical model made with data from *Jorgensen et al.* [1992] for a recharge zone. This is accomplished by taking the sum of the sulfate reduction over the entire vertical profile from the *Jorgensen et al.* [1992] data and dividing by the sulfate reduction rate per m^3 of ridge from *Bach and Edwards* [2003]. By doing this, the data from Guaymas Basin is shown to be around 9 orders of magnitude higher

than the estimate using free energy. From here, each point in Figure 3.4 is reduced by 9 orders of magnitude and then the concentration profiles are recalculated.

The theoretical concentration profiles are shown in Figure 3.9 for a range of flow speeds. The concentration profiles match fairly well with the *Bach and Edwards* [2003] data. For a flow speed of 10^{-10} m/s, the theoretical result shows about 1.3% of the sulfate transported is reduced biogenically whereas for the free energy model, it shows around 2.2%. The general trend of higher flow rates equates with a lower percentage of sulfate reduced holds for both models, and at very high flow rates, both models show biogenic sulfate reduction is negligible.

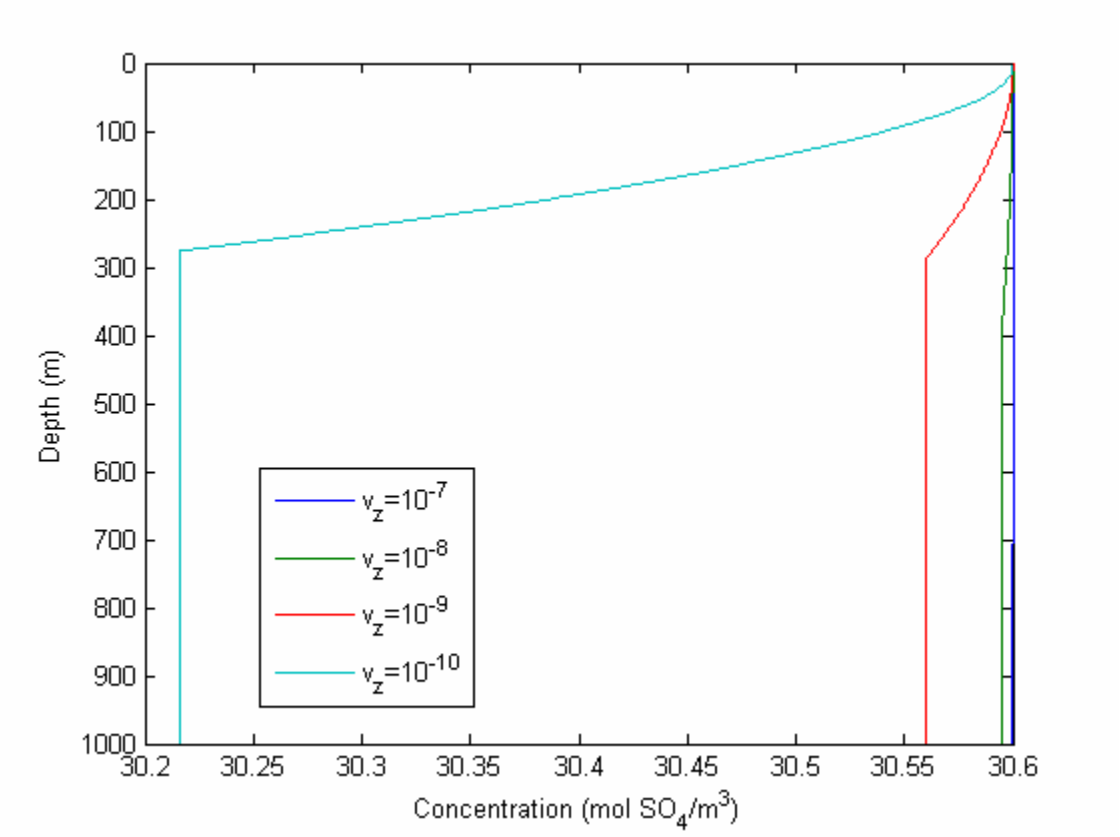

Figure 3.9: Concentration profiles for model formulated from data by *Jorgensen et al.* [1992], reduced by 9 orders of magnitude.

3.3.2: Role of Diffusion

Sulfate in marine sediments has an effective diffusivity of $D_p \sim 5 \times 10^{-10}$ m^2/s [*Krom and Berner*, 1980] and in cracked chalk, its diffusivity is $Dp \sim 0.28\text{-}1.47 \times 10^{-10}$ m^2/s [*Hill*, 1984], which is fairly low, but cannot be ignored when considering flow rates less than 10^{-10} m/s and thin diffusive boundary layers. For very low flow rates, this system would be diffusion dominated and the advective term in Equation 3.5 can be neglected. This system will then scale as

$$\frac{C - C_i}{z^2} \sim \frac{SRR}{D_p} \tag{3.11}$$

To find out how important diffusion is to the system, advective and diffusive time scales need to be found for each flow rate. The value of the length scale, z, will depend directly upon the distance it takes the fluid to reach 110 ^{o}C, which is the threshold temperature for sulfate reducers. The ratio of the advective to diffusive times is

$$\frac{\tau_A}{\tau_D} = \frac{D_p}{v_z z} \tag{3.12}$$

The advective and diffusive times for flow rates between 10^{-7} and 10^{-13} m/s is shown in Table 3.1. The advective time is much shorter than the diffusive time until the flow speed is on the order of $\sim 10^{-12}$ m/s. For the sake of the sulfate reduction model presented in Section 3.2, the

effects of diffusion can be completely neglected due to the fact that advection dominates by many orders of magnitude at the flow speeds considered.

Table 3.1: Summary of advective and diffusive timescales for various flow speeds

Flow Speed, v_z (m/s)	Length Scale(m)	Advective Time (s)	Diffusive Time (s)	τ_a/τ_d
1.00×10^{-7}	871	8.71×10^{9}	7.58641×10^{15}	0.000001
1.00×10^{-8}	387	3.87×10^{10}	1.49769×10^{15}	0.000026
1.00×10^{-9}	286	2.86×10^{11}	8.1796×10^{14}	0.000350
1.00×10^{-10}	276	2.76×10^{12}	7.6176×10^{14}	0.003623
1.00×10^{-11}	275	2.75×10^{13}	7.5625×10^{14}	0.036364
1.00×10^{-12}	275	2.75×10^{14}	7.5625×10^{14}	0.363636
1.00×10^{-13}	275	2.75×10^{15}	7.5625×10^{14}	3.636364

3.3.3: Anhydrite Precipitation

The precipitation of anhydrite in recharge zones is very important to hydrothermal fluid dynamics and can affect the overall permeability structure of the system. *Lowell and Yao* [2002] present a simple single-pass model for anhydrite precipitation with a constant flow rate and they find that for a flow speed in the recharge zone of 10^{-6} m/s, the porosity of the system will be filled up after 680 years. They also show that for the flow speed, each order of magnitude higher or lower results in an inversely proportional sealing time such that for a flow speed of 10^{-5} m/s, the sealing time is on the order 10 years. In terms of bacterial sulfate reduction, the flow speeds that provide for the highest rates of sulfate reduction are also the speeds at which precipitation of anhydrite is negligible in the recharge zones because the sealing times would be on the order of hundreds of thousands of years due to the massive aerial extent of the recharge zones, which is probably many orders of magnitude larger than the maximum lifespan for a hydrothermal system with the obvious exception of the Trans-Atlantic Geotraverse (TAG) hydrothermal mound on the

Mid-Atlantic Ridge, which is around 100 ka [*Rona et al.*, 1986]. This creates a unique situation. The importance of biological sulfate reduction has been suggested as a possible solution to recharge zone sizes. Some models and chemical data require that the recharge regions must be small and the flow speed must be high due to isotopic signatures. This situation would, however, result in the precipitation of a tremendous amount of anhydrite, sealing porosity fairly quickly, and destroying the hydrothermal system. These are the models that would benefit the most from significant biological sulfate reduction, because the microorganisms could remove the sulfate, thus alleviating the impending anhydrite precipitation problem. Alternatively, if the recharge area is large, the flow rates are slower and the rate of precipitation of anhydrite decreases. But the larger recharge area and slower recharge velocity in turn leads to a much higher rate of biological sulfate reduction. This higher sulfate reduction rate results in less sulfate being available for the precipitation of anhydrite and hence the possible reduction of porosity resulting from anhydrite precipitation is further alleviated.

3.4: Conclusions

Biogenic sulfate reduction at fast flow speeds at ridge crest hydrothermal systems is almost negligible whereas slower speeds could allow for a sizable fraction of the transported sulfate to be reduced biogenically. The sulfate reduction rate obtained by *Bach and Edwards* [2003] represents a global average for sulfate reduction along mid-ocean ridge flanks calculated by using the free energy being input into all oceans, and therefore, in some areas, biological sulfate reduction could consume a much larger percentage of the sulfate transported into the oceanic crust at hydrothermal recharge zones. This average value is much smaller than the value for sulfate reduction found at the Guaymas Basin hydrothermal system. This is predominately

due to the high sedimentation rate as well as the massive influx of organic matter and nutrients into the sediments. The data obtained from Guaymas Basin was also performed under laboratory conditions with sediment cores from the site, potentially skewing the results even further. The data at Guaymas Basin came from a hydrothermal upflow zone with a relatively thin thermal boundary layer. The thin boundary layer allows for much less sulfate to be reduced in the Guaymas Basin experiments. The experiments were performed in the presence of high sulfate concentrations and potentially no limit on the amount of H_2, which is commonly the limiting factor in biogenic sulfate reduction. The sulfate reduction rate curves obtained at Guaymas Basin may also be skewed towards the higher temperatures because the microorganisms living at the higher temperatures receive the influx of nutrients first. Nonetheless, the general trend for sulfate reduction was the same for both the Guaymas Basin and the Gibbs free energy calculations in that higher flow speeds resulted in lower sulfate reduction rates and lower flow speeds resulted in higher sulfate reduction rates. The laboratory estimates of the temperature-dependent biogenic sulfate reduction rate appears to be at least two orders of magnitude too high when applied recharge zones within the Guaymas Basin as characterized by Sites 478 and 481. These estimates appear to be as much as nine orders of magnitude too high biogenic sulfate reduction during hydrothermal recharge at mid-ocean ridges.

When the flow speed is low, the precipitation of anhydrite may not be important because most of the seawater sulfate has time to be utilized by microorganisms and a long time is needed to seal porosity as a result of anhydrite precipitation. Likewise, when the flow speed is high, the high local thermal gradient near the base of the recharge zone will result in more sulfate being precipitated as anhydrite. Conversely, the effect of biogenic sulfate reduction will be small because of the short residence time along the flow path. The effect of diffusion is still unclear

because diffusion could be dominant in systems where the boundary layer is very thin, thus allowing for all sulfate to be reduced at any given flow rate. For recharge zones typically thought to characterize mid-ocean ridge hydrothermal systems, the effect of diffusion on the fraction of seawater sulfate reduced is negligible compared to the effect of advection. In the case of discharge or very fast moving recharge zones, diffusion might be dominant in thin boundary layers. This could mean that the amount of sulfate reduction estimated for the Guaymas Basin sediments is actually underestimated because the diffusive boundary layer is not taken into account.

CHAPTER 4

CONCLUSIONS AND RECOMMENDATIONS

Our understanding of deep-sea hydrothermal systems is fairly incomplete and the number of quantitative biological measurements is severely lacking. As of 2004, only about 20% of the predicted ~1000 active vents fields have been explored, and the number that have been studied in detail is significantly lower than that [*Baker and German*, 2004]. To obtain a better understanding of the biogeochemical cycles taking place at the active vents as well as in the subsurface, chemical records need to be taken at regular intervals, if not continuously, for entire eruption cycles. The studies at Axial seamount on the JDF and the EPR 9^{o}N site have been more thorough than most, but still are fairly incomplete. In addition to continued chemical measurements at the sites, heat flow measurements are needed at both high temperature vents and the coupled diffuse flow systems to better constrain flow rates used to model biogeochemical cycles. Better methods for locating and quantifying recharge zones need to be developed to understand the overall fluid dynamics of the hydrothermal system and to model the subsurface biosphere with better accuracy. Drilling techniques need to be developed so the structure of the entire hydrothermal system can be better understood.

When the subsurface biosphere is better understood, the models presented herein can be used to understand numerous processes that take place at hydrothermal systems. If chemical data for coupled high temperature and diffuse flow hydrothermal vents can be obtained for numerous sites over many eruptive cycles, knowledge of the true makeup of 'snowblower' events can be found as well as changes in the porosity of the diffuse flow system. This also

requires much better heat flow measurements over a long period of time for individual vents to be made so that the transport of chemical species through the system can be better constrained. With better heat flow data, more thorough models can be created to quantify recharge zones with much higher accuracy. With this information, the comparative roles of anhydrite precipitation and biological sulfate reduction during hydrothermal recharge can potentially be resolved. Drilling into the hydrothermal systems will resolve all of these problems by helping to quantify population sizes of microorganisms, visualize the extent of anhydrite precipitation, and potentially locate regions of higher and lower permeability for analysis of recharge zones.

Future work in mathematical modeling of biological sulfur reactions at deep-sea hydrothermal systems is still very new, and hence much work is still needed to understand the dynamics of the systems. Most biological work done at hydrothermal vents today involves trying to understand the large animal communities and the symbiotic relationships that exist or to culture new and exciting microorganisms that stretch our imaginations about the extremes life can exist in. Parallels can potentially be drawn between biogenic industrial processes and deep-sea hydrothermal systems. Biofilm kinetics in bioreactors has been a very hot topic for mathematicians and biologists for the past few decades because of the usefulness in sanitation and public health. The subsurface biosphere essentially operates under the same principles, but with much lower nutrient fluxes and in a more extreme environment. The possibilities for new discoveries are large and our understanding of these biological systems is changing at an unprecedented rate. The work presented here on biological sulfur reactions can be interpreted in many different ways depending upon the available data utilized, and as the data become most abundant, perhaps better conclusions can be reached.

REFERENCES

Alt, J.C., J. Holnnorez, C. Laverne and R. Emmermann, Hydrothermal alterations of a 1 km section through the upper oceanic crust, deep sea drilling project hole 504B: mineralogy, chemistry, and evolution of seawater-basalt interactions*, J. Geophys. Res.*, 91, 10309 10336, 1986.

Alt, J.C., Sulfur isotopic profile through the oceanic crust: Sulfur mobility and seawater-crustal sulfur exchange during hydrothermal alteration, *Geology*, 23, 585-588, 1995.

Bach, W. and K.J. Edwards, Iron and sulfide oxidation within the basaltic ocean crust: Implications for chemolithoautotrophic microbial biomass production, *Geochim. Cosmochim. Acta*, 67, 3871-3887, 2003.

Baker, E.T. and C.R. German, On the global distribution of hydrothermal vent fields, in: *Mid-Ocean Ridges: Hydrothermal Interactions Between the Lithosphere and Oceans,* Geophys. Monogr. Ser., vol. 148, edited by C.R. German, J. Lin and L.M. Parson, pp. 245-266, AGU, Washington, D.C., 2004.

Baross, J.A. and S.E. Hoffman, Submarine hydrothermal vents and associated gradient environments as sites for the origin and evolution of life, *Orig. Life*, 15, 327-345, 1985.

Bejan, A., *Convection Heat Transfer*, 2nd ed., John Wiley & Sons, New York, 623 pp., 1995.

Bottcher, M.E., B. Khim, A. Suzuki, M. Gehre, U.G. Wortmann and H. Brumsack, Microbial sulfate reduction in deep sediments of the Southwest Pacific (ODP Leg 181, Sites 1119-1125): evidence from stable sulfur isotope fractionation and pore water modeling, *Marine Geology*, 205, 249-260, 2004.

Canfield, D.E. and D.J. Des Marais, Aerobic sulfate reduction in microbial mats, *Science*, 251, 1471-1473, 1991.

Chevaldonne, P. and A. Godfroy, Enumeration of microorganisms from deep-sea hydrothermal chimney samples, *FEMS Microbiol. Lett.*, 146, 211-216, 1997.

Chyba, C.F., Energy for microbial life on Europa, *Nature*, 403, 381-382, 2000.

Chyba, C.F. and C.B. Phillips, Possible ecosystems and the search for life on Europa, *PNAS*, 98, 801-804, 2001.

Corliss, J.B., J. Dymond, L.I. Gordon, J.M. Edmond, R.P. Von Herzen, R.D. Ballard, K. Green, D. Williams, A. Bainbridge, K. Crane and T.H. Van Andel, Submarine thermal springs on the Galapagos Rift, *Science*, 203, 1073-1083, 1979.

Corliss, J.B., J.A. Baross and S.E. Hoffman, An hypothesis concerning the relationship between submarine hot springs and the origin of life on Earth*, Oceanol. Acta*, 4, 59-69, 1981.

Crowell, B.W., R.P. Lowell and K.L. Von Damm, A model for the production of sulfur floc and "snowblower" events at mid-ocean ridges, *Geochem. Geophys. Geosystems*, (submitted), 2007.

Delaney, J.R., D.S. Kelley, M.D. Lilley, D.A. Butterfield, J.A. Baross, W.S.D. Wilcock, R.W. Embley and M. Summit, The quantum event of oceanic crustal accretion: impacts of diking at mid-ocean ridges, *Science*, 281, 222-230, 1998.

Elsgaard, L., D. Prieur, G.M. Mukwaya and B.B. Jorgensen, Thermophilic sulfate reduction in hydrothermal sediment of Lake Tanganyika, East Africa, *App. Environ. Microbiol.*, 60, 1473-1480, 1994.

Embley, R.W. and W.W. Chadwick, Jr., Volcanic and hydrothermal processes associated with a recent phase of seafloor spreading at the northern Cleft segment: Juan de Fuca Ridge*, J. Geophys. Res*., 99, 4741-4760, 1994.

Embley, R.W., W.W. Chadwick, Jr., I.R. Jonasson, D.A. Butterfield and E.T. Baker, Initial results of the rapid response to the 1993 CoAxial event: Relationships between hydrothermal and volcanic processes, *Geophys. Res. Lett.*, 22, 143-146, 1995.

Fisher, A.T., Permeability within basaltic oceanic crust, *Rev. Geophys.*, 36, 143-182, 1998.

Fisher, A.T., E.E. Davis, M. Hutnak, V. Spiess, L. Zuhlsdorff, A. Cheraoui, L. Christiansen, K.M. Edwards, R. Macdonald, H. Villinger, M.J. Mottl, C.G. Wheat and K. Becker, Hydrothermal recharge and discharge across 50 km guided by seamounts on a young ridge flank, *Nature*, 421, 618-621, 2003.

Fornari, D., M. Tivey, H. Schouten, M. Perfit, D. Yoerger, A. Bradley, M. Edwards, R. Haymon, D. Scheirer, K. Von Damm, T. Shank and A. Soule, Submarine lava flow emplacement at the East Pacific Rise 9^{o} 50'N: Implications for uppermost ocean crust stratigraphy and hydrothermal fluid circulation, in: *Mid-Ocean Ridges: Hydrothermal Interactions Between the Lithosphere and Oceans,* Geophys. Monogr. Ser., vol. 148, edited by C.R. German, J. Lin and L.M. Parson, pp. 187-218, AGU, Washington, D.C., 2004.

Haymon, R.M., D.J. Fornari, K.L. Von Damm, M.D. Lilley and M.R. Perfit, Volcanic eruption of the mid-ocean ridge along the east Pacific Rise crest at 9° 45' -52'N: direct submersible observations of seafloor phenomena associated with an eruption event in April, 1991, *Earth Planet. Sci. Lett*., 119, 85-101, 1993.

Heijnen, J.J. and J.P. Van Dijken, In search of a thermodynamic description of biomass yields for the chemotrophic growth of microorganisms, *Biotechnol. Bioengineer.*, 39, 833-858, 1992.

Hill, D., Diffusion coefficients of nitrate, chloride, sulphate and water in cracked and uncracked chalk, *European J. Soil Sci.*, 35, 27-33, 1984.

Holden, J.F., M. Summit and J.A. Baross, Thermophilic and hyperthermophilic micro organisms in 3-30°C fluids following a deep-sea volcanic eruption. *FEMS Microbiol. Ecol.*, 25, 33-41, 1998.

Huber, J.A., D.A. Butterfield and J.A. Baross, Bacterial diversity in a subseafloor habitat following a deep-sea volcanic eruption, *FEMS Microbiol. Ecol.*, 43, 393-409, 2003.

Huber, R., P. Stoffers, J.L. Cheminee, H.H.Richnow and K.O. Stetter, Hyperthermophilic archaebacteria within the crater and open-sea plume of erupting MacDonald Seamount, *Nature*, 345, 179-182, 1990.

Ingvorsen, K., J.G. Zeikus and T.D. Brock, Dynamics of bacterial sulfate reduction in a eutrophic lake, *App. Environ. Microbiol.*, 42, 1029-1036, 1981.

Jannasch, H.W., Review lecture: The chemosynthetic support of life and the microbial diversity at deep-sea hydrothermal vents, *Proc. R. Soc. London Ser. B*, 225, 277 297, 1985.

Jannasch, H.W. and M.J. Mottl, Geomicrobiology of deep-sea hydrothermal vents, *Science*, 229, 717-725, 1985.

Jannasch, H.W., D.C. Nelson and C.O. Wirsen, Massive natural occurrence of unusually large bacteria (Beggiatoa sp.) at a hydrothermal deep-sea vent site, *Nature*, 342, 834-836, 1989.

Jorgensen, B.B., Mineralization of organic matter in the sea bed – the role of sulphate reduction, *Nature*, 296, 643-645, 1982.

Jorgensen, B.B. and F. Bak, Pathways and microbiology of thiosulfate transformations and sulfate reduction in a marine sediment (Kattegat, Denmark), *App. Environ. Microbiol.*, 57, 847-856, 1991.

Jorgensen, B.B., M.F. Isaksen and H.W. Jannasch, Bacterial sulfate reduction above 100

degrees C in deep-sea hydrothermal vent sediments, *Science*, 258, 1756-1757, 1992.

Juniper, S.K., P. Martineau, J. Sarrazin and Y. Gelinas, Microbial-mineral floc associated with nascent hydrothermal activity on CoAxial segment, Juan de Fuca mid-ocean ridge, *Geophys. Res. Lett.*, 22, 179-182, 1995.

Kaksonen, A.H., J.J. Plumb, W.J. Robertson, S. Spring, P. Schumann, P.D. Franzmann and J.A. Puhakka, Novel thermophilic sulfate-reducing bacteria from a geothermally active underground mine in Japan, *App. Environ. Microbiol.*, 72, 3759-3762, 2006.

Kallmeyer, J. and A. Boetius, Effects of temperature and pressure on sulfate reduction and anaerobic oxidation methane in hydrothermal sediments of Guaymas Basin, *Appl. Environ. Microbiol.*, 70, 1231-1233, 2004.

Kelley, D.S., J.A. Baross and J.R. Delaney, Volcanoes, fluids, and life at mid-ocean ridge spreading centers, *Annu. Rev. Earth Planet. Sci*., 30, 385-491, 2002.

Knoblauch, C. and B.B. Jorgensen, Effect of temperature on sulphate reduction, growth rate and growth yield in five psychrophilic sulphate-reducing bacteria from Arctic sediments, *Environ. Microbiol.*, 1, 457-467, 1999.

Krom, M.D. and R.A. Berner, The diffusion coefficients of sulfate, ammonium and phosphate ions in anoxic marine sediments, *Limnol. Oceanogr.*, 25(2), 327-337, 1980.

Lowell, R.P., Modeling continental and submarine hydrothermal systems, *Rev. Geophys.*, 29, 457-476, 1991.

Lowell, R.P., P.A. Rona and R.P. Von Herzen, Seafloor hydrothermal systems, *J. Geophys. Res.*, 100, 327-352, 1995.

Lowell, R.P. and L.N. Germanovich, Evolution of a brine-saturated layer at the base of a ridge-crest hydrothermal system, *J. Geophys. Res.*, 102, 10,245-10,255, 1997.

Lowell, R.P. and Y. Yao, Anhydrite precipitation and the extent of hydrothermal recharge zones at ocean ridge crests*, J. Geophys. Res.*, 107 (B9), 2183, doi: 10.1029/2001JB001289, 2002.

Lowell, R.P., Y. Yao and L.N. Germanovich, Anhydrite precipitation and the relationship between focused and diffuse flow in seafloor hydrothermal systems, *J. Geophys. Res.*, 108 (B9), 2424, doi: 10.1029/2002JB002371, 2003.

Lowell, R.P. and L.N. Germanovich, Hydrothermal processes at mid-ocean ridges: Results from scale analysis and single-pass models, in: *Mid-Ocean Ridges:*

Hydrothermal Interactions between the Lithosphere and Oceans, Geophys. Monogr. Ser., vol. 148, edited by C.R. German, J. Lin and L.M. Parson, pp. 219 244, AGU, Washington, D.C., 2004.

Lowell, R.P., B.W. Crowell, K.C. Lewis, and L. Liu, Modeling multiphase, multi-component processes at oceanic spreading centers: Magma to microbe, in *Modeling Hydrothermal Processes at Oceanic Spreading Centers*: *Magma to Microbe*, *Geophys. Monogr. Ser.*, *xxx*, ed. by R.P. Lowell, J.S. Seewald, M.R. Perfit, and A. Metaxas, p. xxx, American Geophys. Union, Washington, DC (submitted), 2007a.

Lowell, R.P., S.R. Gosnell and Y. Yang, Numerical simulations of single-pass hydrothermal convection at mid-ocean ridges: Effects of the extrusive layer and temperature-dependent permeability, *Geochem. Geophys. Geosystems*, (in revision), 2007b.

McKay, C.P. and H.D. Smith, Possibilities for methanogenic life in liquid methane on the surface of Titan, *Icarus*, 178, 274-276, 2005.

Nelson, D.C., R.M. Haymon and M.D. Lilley, Rapid growth of unusual hydrothermal bacteria observed at new vents during AdVenture dive program to the EPR at 9˚45' -52'N, *Eos Trans. Am. Geophys. Union*, 72, 481, 1991.

Phillips, O.M., *Flows and Reactions in Permeable Rocks*, Cambridge University Press, Cambridge, UK, 285 pp., 1991.

Ramondenc, P., L.N. Germanovich, K.L. Von Damm and R.P. Lowell, The first measurments of hydrothermal heat output at 9°50'N, East Pacific Rise, *Earth Planet. Sci. Lett.*, 245, 487-497, 2006.

Rona, P.A., G. Klinkhammer, T.A. Nelson, J.H. Trefry and H. Elderfield, Black smokers, massive sulfides and vent biota on the Mid-Atlantic Ridge, *Nature*, 321, 33-37, 1986.

Seyfried, W.E., Jr., and J.L. Bischoff, Low temperature basalt alteration by seawater: an experimental study at 70C and 150C, *Geochim. Cosmochim. Acta*, 43, 1937-1947, 1979.

Seyfried, W.E., Jr., and M.J. Mottl, Hydrothermal alterations of basalt by seawater under seawater-dominated conditions, *Geochim. Cosmochim. Acta,* 46, 985-1002, 1982.

Shank, T.M., D.J. Fornari, K.L. Von Damm, M.D. Lilley, R.M. Haymon and R.A. Lutz, Temporal and spatial patterns of biological community development at nascent deep-sea hydrothermal vents 9°50'N, East Pacific Rise), *Deep-Sea Res.*, 45, 465 515, 1998.

Shank, T.M., B. Govenar, K. Buckman, D.J. Fornari, S.A. Soule, G.W. Luther, R.A. Lutz, C. Vetriani, M. Tolstoy, R.H. Rubin, J.P. Cowen and K.L. Von Damm, Initial Biological, Chemical and Geological Observations After the 2005-6 Volcanic Eruption on the East Pacific Rise, *Eos Trans. AGU*, 87(52), Fall Meet.

Suppl., Abstract V13C-04, 2006.

Sorensen, K.B., K. Finster and N.B. Ramsing, Thermodynamic and kinetic requirements in anaerobic methane oxidizing consortia exclude hydrogen, acetate, and methanol as possible electron shuttles, *Microb. Ecol.*, 42, 1-10, 2001.

Taylor, C.D. and C.O. Wirsen, Microbiology and ecology of filamentous sulfur formation, *Science*, 277, 1483-1485, 1997.

Taylor, C.D., C.O. Wirsen and F. Gaill, Rapid microbial production of filamentous sulfur mats at hydrothermal vents, *Appl. Environ. Microbiol*., 65, 2253-2255, 1999.

Van Dover, C.L. and R.A. Lutz, Experimental ecology at deep-sea hydrothermal vents: a perspective, *J. Exper. Marine Biol. Eco.*, 300, 273-307, 2004.

Von Damm, K.L., Chemistry of hydrothermal vent fluids from 9^{o}-10^{o}N, East Pacific Rise: "Time zero," the immediate posteruptive period*, J. Geophys. Res.*, 105, 11,203-11,222, 2000.

Von Damm, K.L. and M.D. Lilley, Diffuse flow hydrothermal fluids from 9°50'N East Pacific Rise: Origin, evolution and biogeochemical controls, in: *The Subsurface Biospere at Mid-Ocean Ridges*, Geophys. Monogr. Ser., vol. 144, edited by W.S.D. Wilcock, E.F. DeLong, D.S. Kelley, J.A. Baross and S.C. Cary, pp. 245 268, AGU, Washington, D.C., 2004.

Wirsen, C.O., S.M. Sievert, C.M. Cavanaugh, S.J. Molyneaux, A. Ahmad, L.T. Taylor, E.F. DeLong and C.D. Taylor, Characterization of an autotrophic sulfide oxidizing Arcobacter sp. that produces filamentous sulfur, *Appl. Environ. Microbiol*., 68, 316-325, 2002.